TECHNICAL MEMORANDUM

315

Intercomparison of the performance of operational ocean wave forecasting systems with buoy data

J-R. Bidlot, D.J. Holmes, P.A. Wittmann,
R. Lalbeharry and H.S. Chen

Research Department

September 2000

European Centre for Medium-Range Weather Forecasts
Europäisches Zentrum für mittelfristige Wettervorhersage
Centre européen pour les prévisions météorologiques à moyen

Intercomparison of the performance of operational ocean wave forecasting systems with buoy data

Jean-Raymond Bidlot[1], Damian J. Holmes[2], Paul A. Wittmann[3], Roop Lalbeharry[4], Hsuan S. Chen[5]

[1] ECMWF, Shinfield Park, Reading, UK;

[2] Ocean Application Branch, Meteorological Office, Bracknell, UK;

[3] Models and Data Department, Fleet Numerical Meteorology and Oceanography Center, Monterey, CA, USA;

[4] Meteorological Research Branch, Atmospheric Environment Service, Downsview, Ontario, Canada

[5] National Centers for Environmental Prediction, Camp Springs, MD, USA

Abstract

Since the end of 1995, a monthly exchange of ocean wave model data has been taking place between five operational weather centres. The data are compared to observations obtained from moored buoys and platforms as reported via the GTS. Observations of wind speed, wave height and peak period are set against model analyses and forecasts. Three years of data are compiled here using basic statistics and time series comparison. This exchange of information has allowed a comparison of the various operational ocean wave forecasting systems (winds and waves) with the identification of areas for their potential improvements. The sensitivity of wave model results to the quality of the forcing wind fields is reiterated.

1. Introduction

Any operational weather centre involved in wave prediction should have some form of quality monitoring of their products. For quite some time now, operational weather centres have systematically exchanged statistical information (scores) in an attempt to further diagnose the quality of their atmospheric model, however prior to the end of 1995, no systematic comparative study of the different wave forecasting systems existed.

In the past, there has been some efforts to evaluate the quality of hindcast wave products. This is particularly true when new model developments took place. The typical performance of early global wave models was summarized by *Cardone* (1987), *Zambresky* (1987, 1989), and *Clancy et al.* (1986). More recent evaluations of the operational performance of the third generation wave model (WAM) can be found in *Khandekar and Lalbeharry* (1996), *Wittmann et al.* (1995) and *Janssen et al.* (1997a). In an attempt to derive as much information as possible on their system, Janssen et al. have also used ERS-1 altimeter data. Moreover, they have compared forecasts with the corresponding analyses by introducing similar scores as used for atmospheric fields.

Satellite data are another valuable source of wave observations, albeit not always independent and with errors which are harder to understand. Earlier work by *Romeiser* (1993) and the more recent comprehensive study of Bauer et al. (1998) have nevertheless shown the relative good quality of both model and the latest satellite data (Topex, ERS).

The combined use of in situ (buoys) and satellite wave observations has now become a usual diagnostic tool of surface winds via the integrating effect of a wave model. For example, the quality of the surface winds from the ECMWF 15 year reanalysis (ERA) was examined by forcing the model WAM with those winds (*Sterl et al.* 1998) and comparing the results to buoy and altimeter data. It is also done on a more routine basis for the monitoring of the ECMWF forecasting system (*Janssen et al.* 2000).

A systematic comparison of wave model results with other models is not often reported. It is usually confined to the initial phase of a new model implementation or when different models are compared in order to select one for operational production. In 1995, as a first step towards a more comprehensive comparison of operational wave forecasting systems, a group of wave modellers from different meteorological centres agreed to exchange wave model results (analyses and forecasts) at selected locations for which wave and surface wind information can easily be obtained. This exercise provided the participants with an extra diagnostic tool for their forecasting system. The methodology and preliminary results of this data exchange were illustrated in *Bidlot et al.* (1998) and *Bidlot and Holt* (1999). In this follow-up paper, the evaluation of data obtained from a three year period (December 1996 to December 1999) is presented.

Five centres are currently participating in the comparison. The implementation of their wave forecasting system is briefly described in section 2. The wind and wave observations are obtained from moored buoys and fixed platforms for which data are made available to the meteorological community via the global telecommunication system (GTS). The required data processing of these observations is summarised in section 3. Results from the statistical comparison are presented in section 4. Section 5 comments on some of the aspects that were illustrated in the previous sections. Then conclusions stressing the need for the continuation and development of this data exchange.

2. Wave models

In late 1995, the European Centre for Medium-range Weather Forecasts (ECMWF), the United Kingdom Meteorological Office (UKMO), the Fleet Numerical Meteorology and Oceanography Center (FNMOC), and the Atmospheric Environment Service (AES), now called the Meteorological Service of Canada (MSC), started a project aimed at exchanging wind and wave model data at given geographical points. They were joined, in May 1996, by the National Centers for Environmental Prediction (NCEP). Apart from a different atmospheric model used to produce the necessary surface wind forcing, each centre has a different wave model and/or a different implementations of the same original model. A basic description of each system is given below and is also summarised in table 1.

2.1 The ECMWF wave model

The third generation wave model WAM was developed in the mid 80's by an international group of wave modellers (*Komen et al.*, 1994). It has been installed at many institutions around the world. At ECMWF, the WAM model is in constant evolution. Currently it is implemented for two regions (*Janssen et al.* 1997a, *Bidlot et al.* 1997). In the global version, the discretised wave spectrum has 25 logarithmically spaced frequency bins (from 0.0418 Hz to 0.411 Hz) and 12 directional bins. The limited area model uses the same number of frequencies but 24 directions. Since May 1997, the first direction is no longer zero but half the directional bin width in order to avoid the streaking problem which occurs when spurious wave energy propagates along longitude or latitude (*Bidlot et al.* 1997). It also alleviates shadowing problems behind islands. Shallow water physics such as shoaling and bottom dissipation are included in both models.

The parallel version of the global model was introduced in December 1996. It has an effective resolution of the order of 55 km by making use of an irregular lat-lon grid (*Bidlot and Holt* 1999). It extends from 81°S to 81°N and covers all major water bodies. A higher resolution model is also run for the whole North Atlantic, the North Sea, the Mediterranean Sea and the Black Sea with an effective resolution of the order of 27 km on

an irregular lat-lon grid. Sea surface temperature analysis is used to determine the sea ice coverage where wave energy is set to zero.

Before July 1998, only one daily 10 day global wave forecast was obtained starting from the 12Z analysis and forced by 10m winds at 6 hourly intervals from the ECMWF atmospheric model output (*Bengtson* 1999, *Janssen et al.* 1997a). The analysis was obtained from the previous one by running the wave model with analysed 10m winds and blending the model data with ERS satellite altimeter wave height observations. The scheme is based on the optimum interpolation scheme developed by *Lionello et al.* (1992). During this period, changes to the atmospheric model were also made. Generally, those modifications were found to have positive impacts on the quality of the surface winds and thus on the waves (*Janssen et al.* 2000), notably the introduction of a reformulation of the background error covariance in the variational scheme in May 1997 (*Derber and Bouttier* 1999), and the operational implementation of the four dimensional variational analysis method (4dvar) in December 1997 (*Rabier et al.* 1999, *Mahfouf and Rabier* 2000).

Since June 29 1998, the wave model has been directly coupled to the atmospheric model (*Janssen et al.* 2000a). In this configuration, updated winds are provided hourly to the wave model subroutine which returns an update to the atmospheric model of the ocean roughness via a Charnock parameter field. This feedback is intended to model the effect of wave generation on surface stress (*Janssen* 1989, 1991) and was shown to be beneficial in improving global forecast scores (*Janssen et al.* 2000b, *Janssen* 2000) as well as climate based runs (*Janssen and Viterbo* 1996). Two forecasts are produced daily from the 12Z analysis and from the 0Z short cut-off analysis, however, only forecasts based on the 12Z analysis are disseminated to users.

The ECMWF ensemble prediction system (*Buizza et al.* 1999) is also run with a coupled wave model, albeit with a coarser resolution of 1.5°x1.5° and only deep water physics. Information on the probability of wave forecasts can be derived with potential use such as in ship routing (*Hoffschildt et al.* 1999). The daily limited area wave model forecasts are only produced from the 12Z analysis and extend to 5 days. 10m archived winds at 6 hourly intervals are used to force the model.

Finally in June 1999, a revised formulation of the wave integration scheme became operational along with a correction to the altimeter wave height data for non Gaussian sea state (*Janssen* 1999, 2000). Note that the wave spectral resolution was later increased to 24 directions and 30 frequencies in November 2000.

2.2 The UK Met Office wave model

The operational wave model run at the Met Office is a second generation model based on the wave model first developed and described by *Golding* (1983), although there has been a continuous program of development since its initial implementation (*Holt* 1994). The wave energy spectrum is divided into 13 frequency components and 16 direction components. The lowest model frequency is 0.04Hz (corresponding to waves of 25 seconds period and wavelength 975m), while the highest is 0.324Hz (3 seconds period, wavelength about 15m). Intermediate frequencies are spaced logarithmically while the effect of waves at higher frequencies is included in the calculation of source terms.

The Met Office model is run over three areas. All models include the effects of shallow water and take hourly wind data from the appropriate NWP atmosphere model run.

The global model covers 80.28°N to 79.72°S on a regular latitude-longitude grid, at a resolution of 0.833° longitude by 0.556° latitude. The model run consists of a 12 hour hindcast, during which assimilation of ERS-2 radar altimeter measurements of significant wave height is performed, followed by a 5 day forecast. Sea-ice coverage is updated daily, with data coming from the NWP sea-ice analysis. Hourly boundary data is provided for both of the regional models. The model is run twice daily following the midnight and midday runs of the NWP global atmosphere model.

The coarser of the regional models covers the continental European shelf, including the Mediterranean, Black and Baltic Seas, at a resolution of 0.4° longitude by 0.25° latitude. This model also runs twice daily, following the midnight and midday runs of the NWP global preliminary atmosphere model. The run consists of a 12 hour hindcast followed by a 2 day forecast. This is then extended to 5 days using wind data from the global model.

In March 2000, a higher resolution regional model was introduced covering the regions surrounding the UK. This model runs at a resolution of 0.111° latitude by 0.1667° longitude. Wind data are provided by the NWP mesoscale atmosphere model, while the effects of time-varying currents are included, as described by *Buckley* (1999). Hourly current data are provided by The Met Office storm-surge model, which uses the same grid as the wave model and also uses NWP mesoscale surface forcing. The model runs 4 times per day, the run consisting of a 6 hour hindcast followed by a 2 day forecast. It is intended that this will be extended to a 5 day forecast using global model wind data in a similar manner to the European area model.

The Met Office wave data assimilation scheme works in a similar manner to that of ECMWF. Each takes observations of wave height and surface wind speed and calculates the necessary changes to the model wave spectrum, so that the model wave height is 'nudged' closer to the observed value. The Met Office scheme to calculate the wave height changes is based on the 'analysis correction' scheme, while the procedure to transform wave height and wind speed to spectral energy values was developed by *Thomas* (1988). Raw observations are quality controlled (using a background climatology test and 'buddy'-tests) and are then averaged to produce 20-second 'superobs.' After quality control this process produces approximately 1200 superobs from 12 hours of observations (*Holt* 1997).

2.3 The FNMOC wave model

The Fleet Numerical Meteorology and Oceanography Center (FNMOC) employs both global and regional implementations of WAM 4.0. The global implementation runs on a 1.0 degree spherical grid in deep water mode (*Wittmann and Clancy*, 1994). The directional spectrum is represented by 24 directional bins and 25 logarithmically spaced frequency bins (from 0.033 Hz to 0.328 Hz). A satellite derived ice analysis, updated daily, is used to exclude grid points which are covered with ice. The FNMOC global WAM is forced by surface wind stress at 3 hour intervals from the Navy's Operational Global Atmospheric Prediction System (NOGAPS) NWP model (*Hogan and Rosmond*, 1991). Both NOGAPS and WAM run on a 6 hourly update cycle, with forecast runs at 00 GMT and 12 GMT to 144 hours. Currently, the FNMOC WAM does not assimilate wave measurements; the model is initialized from the 3-hour forecast of the previous run.

FNMOC maintains many regional implementations of WAM 4.0, some of which are nested within the global WAM depending on the existence of open ocean boundaries (*Wittmann and Pham*, 1999). These regional implementations run at approximately 27-km resolution and exercise the shallow water physics in WAM.

They are forced by the Coupled Ocean/Atmosphere Mesoscale Prediction System (COAMPS) surface winds (see *Hodur*, 1997). These models run on a 12-hour update cycle and typically forecast to 48 hours. The area coverage and configuration of these

COAMPS/WAM systems change frequently depending on the Navy's priorities.

2.4 The AES WAM-Atmospheric model system

The Canadian Meteorological Centre (CMC) of AES implemented the WAM Cycle-4 in an operational mode in February 1996, replacing the first generation Canadian spectral ocean wave model in operation since December 1990. Two regional versions of the WAM were implemented, one for the northwest Atlantic ocean extending from 25°N to 70°N and from 80°W to 15°W and the other for the northeast Pacific ocean bounded by latitudes 25°N and 60°N and longitudes 160°E and 120°W. Each version has a grid spacing of 1.0° in both latitude and longitude directions and employs deep water physics in the solution of the energy transfer equation for 25 frequencies logarithmically spaced at intervals of $\Delta f/f = 0.1$ from 0.042 Hz to 0.41 Hz and 24 directional bands of 15° each.

Both regional WAM4s were initially driven by winds obtained from the two operational numerical weather prediction models in use at the CMC. The Atlantic WAM4 was originally forced by winds from the regional finite element (RFE) model producing short-range forecasts up to 48 hours. The horizontal grid is a variable resolution grid with a central domain of uniform grid spacing of 50 km covering most of North America and adjacent waters. The vertical discretization consists of 28 σ-levels with the lowest prognostic level being about 40 m above the surface. The regional data assimilation system (RDAS) based on multivariate optimum interpolation was implemented in December 1992 (Chouinard et al. 1994) to provide an analysis at run time following a 12h spin-up cycle initiated from the global data analysis 18 hours earlier, while in December 1995 the RFE model resolution in the central window was increased to 35 km. Details of the RFE model, the changes made to it, and its physical parameterization are described in *Mailhot et al.* (1995, 1997). On the other hand, the Pacific WAM4 was forced by winds generated by the medium range (> 2 days) global spectral finite element (SEF) model. It has a uniform grid spacing of about 0.9° (about 100 km), a spectral representation of 199 waves for the model fields and 21 levels in the vertical (*Ritchie and Beaudoin*, 1994) with the lowest prognostic level being about 80 m above the surface. The SEF model served both as the global data assimilation model and the medium range forecast model.

The Global Environmental Multiscale (GEM) model replaced the RFE model as the regional model on 24 February 1997 without a RDAS. It uses the static analysis from the global SEF model as its initial conditions to produce short-range (up to 2 days) forecasts. The GEM model has a global variable resolution latitude-longitude mesh which can be arbitrarily rotated to permit resolution to be focused over the area of interest and 28 η-levels in the vertical with the lowest prognostic level being about 40 m above the surface. The model can be used in uniform resolution mode for medium range forecasting or in focused mode for short range regional forecasting (Côté et al., 1998a,b). For its initial operational implementation in the regional mode, the GEM model had a grid resolution of 0.33° (about 35 km). On 18 June 1997 a new global 3D variational (3DVAR) analysis (*Gauthier et al. 1999*) replaced the SEF-driven global optimum interpolation analysis, while in September 1997 the 3DVAR data assimilation system was implemented for the GEM regional analyses (*Laroche et al.* 1999). In September 1998, the regional model resolution in the uniform window was increased to 0.22° (about 24 km) and in October 1998, the SEF model was replaced by the global GEM model

with the same uniform grid resolution as the SEF model. This unified system for short-range and medium-range forecasting allows the global cycle and the regional cycle to share the same code, the same physics library, and the same data assimilation system code (*Steenbergen et al.,* 1998). However, the physics options used operationally are not all the same in the two models.

The CMC weather prediction models use the dynamic variables at their lowest prognostic level (80 m for the SEF model and 40 m for the RFE and GEM models), the Monin-Obukov similarity theory for the surface layer, the surface temperature and moisture, and the turbulent kinetic energy in the planetary boundary layer to calculate the fluxes of momentum, heat and moisture at the surface and the variables at the base of the models, nominally at σ or $\eta = 1$ (*Delage* 1997, *Delage and Girard* 1992). The variables at this level are different from those at the surface and represent the winds at the 10 m level and the temperature and moisture at the Stevenson screen level (1.5 m). Over the oceans the surface roughness is given by the Charnock equation (*Charnock*, 1955) in which the Charnock parameter is set to a constant = 0.018 (mature seas) in the RFE and GEM models and 0.032 (younger seas) in the SEF model.

The WAM4 grid is partially covered with sea ice mainly in the winter months. For each run the ice field for input to the WAM4 is obtained from the CMC sea ice analyses. The WAM4 model grid point is considered to be a sea ice point if the ice fraction at that point > 0.5. Once this determination is made at the beginning of each model run, the ice field remains unchanged during the 48-hour forecast period. At all land points, and at all sea ice points, the wave energy of each spectral component is set equal to zero.

2.5 The NCEP Operational Global Ocean Wave Model

Since October 1994, WAM cycle4 has become the NCEP operational global wave model (Chen 1995). The model was modified to accommodate an ever-changing ice edge and to assimilate buoy and ERS-2 Altimeter wave data (since February 1998). In both cases, a successive correction scheme for data assimilation is employed. In this scheme, the significant wave height is replaced by the observed data and the wave spectrum is constructed by assuming the same proportional distribution of wave components of the replaced one. The model was also modified to fix the streaking problem that may occur under a low wind condition when excess spurious wave energy propagates along longitude or latitude. WAM uses the upwind numerical scheme for wave propagation that is more or less the back ray tracing scheme. This scheme generates numerical diffusion to spread energy laterally only for the wave propagating in the direction other than longitude or latitude. Therefore, to fix the streaking problem, the model is simply modified to use three lateral grid points (instead of one point in the WAM code) with the weighing factor 0.92 for the middle point and 0.04 for each side point for the wave propagating only along longitude and latitude, to provide some numerical diffusion for spreading energy laterally.

NOAA/WAM is run twice daily at the 0 and 12Z forecast cycles to produce global ocean wave spectra for a 12-h hindcast and a 3 day forecast. The lowest sigma layer winds from the NCEP analysis and aviation winds (AVN) are adjusted to a height of 10 m by using a logarithmic profile and are used to drive the surface ocean waves. Analysis wind fields from the previous 12 hours at 3-h intervals are used for a 12-h wave hindcast and AVN at 3-h intervals for the wave forecasts. The model grid covers the global ocean from 67.5°S to 77.5°N with a grid resolution of 2.5°. The wave spectrum has 12 directions and 25 logarithmically spaced frequencies.

Note that as the result of a recent instalment of an IBM RS/6000 SP computer system at NCEP, a third generation wave model NWW3 (*Tolman* 1999), that utilizes parallel programming and has different wave physics and differently numerical scheme, has replaced the NOAA/WAM as the NOAA operational global wave model since February 2000.

2.6 Model summary

Table1 summarises the key differences and similarities between the different operational system. All centres use the WAM model cycle 4, except UKMO which has its own second generation wave model. AES actually runs two regional models, one for the North Atlantic and one for the North Pacific with a southern boundary at 25° N. The ECMWF wave model is now coupled to its atmospheric model which supplies surface winds every hour. The other implementation of WAM are forced by winds updated every 3 hours, and the UKMO wave model uses hourly values of surface winds. ECMWF, UKMO, and NCEP incorporate ERS-2 altimeter data in their analysis.

3. Wave and wind data

Sea state and ocean surface meteorological observations are routinely collected by several national organisations via networks of moored buoys and platforms deployed in their near- and offshore regions (the word buoys is used for moored buoys or platforms since their observations are reported under the same WMO header as automatic synop ship). The geographical coverage of the data is still very limited, and at the present wave model resolution, only a small number of all these buoys are within the model grids. Nevertheless, about 40 buoys can be selected which are well within the grid of each model, in relatively deep water as most global wave models are set up as deep water models, and have a high rate of data availability and reliability. Figure 1 shows the location of all buoys used in this comparison.

The buoy data are transferred continuously via the GTS to most national meteorological centres and are usually archived locally. It is therefore a simple matter to build collocations between these observations and the corresponding model values interpolated to the buoy locations. A direct comparison between model values and buoy observations is undesirable as measurements may still contain erroneous data points. Furthermore, model and observed quantities represent different time and spatial scales. From the buoy records, monthly time series are reconstructed and used to perform a basic quality check on the data. This quality check procedure will only keep values that are within acceptable physical range, will try to detect faulty instruments by removing all constant records of one day long or more, and will remove outliers by looking at the deviation from the mean of each monthly data record and from the deviation from one hourly value to the next. Spatial and temporal time scale are made comparable by averaging the hourly observations in time windows of 4 hours centred around the synoptic times. GTS data are unfortunately provided with some truncation. Wave heights are rounded to the closest 0.1 metre, peak frequencies to the closest second and wind speed to the closest meter per second. Averaging will diminish the effect of these truncations. The resulting error for wave data are well within what can be expected from buoy measurements (*Monaldo* 1988). It is however unfortunate that wind speed observations are encoded with such a large truncation error (up to 0.5 m/s).

This quality check procedure is run at ECMWF. For completeness, the ECMWF collocation files also include the raw synoptic unaveraged observations. Other centres build similar buoy-model collocations or have agreed to provide corresponding model values at as many buoy locations as possible (figure 1). Every month,

each participating centre creates files which contain model monthly time series of 10m wind speed and direction, wave height and wave peak period at the selected buoy locations. It was decided to look at the analysis and forecasts up to day 5 (when available, see table 1). These files are transferred via FTP to the UKMO server, where they are combined with the observations processed by ECMWF.

It is the responsibility of each individual centre to retrieve the combined files from the UKMO server. The statistical analysis of the data is left to each centre which may decide to look at it from their own perspective. However, ECMWF has a semi-automatic procedure to analyse the monthly results from which tables and summary graphs are produced. These tables and graphs are also available every month from the UKMO server. The same software can also be used to look at longer periods.

In this paper and in the future, statistics are compiled with quality controlled data supplemented with a blacklisting (omission) of a few data segments. The blacklisting of certain stations is done each month by collecting information from the data providers (web pages, e-mails,...) and by analysing the monthly time series for suspicious behaviours which have eluded the quality control. Note that it was decided to use near real time GTS data instead of data compiled later by the respective data providers, presumed of better quality, since most centres generate their buoy-model collocation when model data are still directly available on-line for immediate comparison.

Buoy anemometers are not usually at a height of 10 metres. However the height of the anemometers has been obtained from the data providers (fig. 1). The wind speed statistics were produced by adjusting the buoy winds to 10m. The steady state neutrally stable logarithmic vertical wind profile relation is solved for the surface stress assuming that the surface roughness can be specified by the Charnock relation with a constant parameter of 0.018 (*Charnock* 1955). The same logarithmic profile is then used to determine the corresponding wind speed at 10m.

4. Data products

4.1 global analysis

Figure 2 shows scatter diagrams of the collocation between all buoy data and model wave heights and wind speed for the 12Z analysis covering a 3 year period (December 1996 to December 1999). The corresponding statistics are summarised in tables 2 and 3. Note that for these plots, only collocation points are considered which were common to the 3 centres which issue 5 day forecasts (i.e. ECMWF, UKMO, FNMOC). AES statistics are produced only with buoys along the continental US and Canada (statistics per region are discussed below). NCEP has slightly fewer data points because of difficulties in getting all collocated data. Also NCEP has been making use of buoy data in their wave model assimilation since February 1998. Similar scatter plots and statistics can be produced for the forecast products. Figure 3 and tables 4 and 5 present the statistics for the day 2 forecast for the same period. From the visual inspection of the scatter diagrams for the analysed wave heights (fig. 2), it appears that among the centres which do not assimilate buoy data, ECMWF had the smallest scatter. However, for this 3 year period, all WAM models have a tendency to underestimate some events, ECMWF in particular. This impression is confirmed by the statistics displayed in tables 2 and 3. ECMWF has indeed the smallest scatter index (standard deviation of the difference between model and buoy normalised by the buoy mean) but was found to have the largest negative bias (model minus buoy) and a symmetric slope less than 1 (the slope of the linear fit where neither the observations nor the model values can

be used as a reference). Not surprisingly, the scatter diagrams for the analysed wind speed generally show a good fit between models and observations. Note however that with the exception of UKMO, all global models have a global small negative bias (recall that the wind speed data were adjusted to a height of 10m).

The scatter diagrams for the day 2 forecast clearly illustrate the degradation of the quality of the forecasts with respect to the analysis, especially for the wind speed (fig. 3). As discussed in *Janssen et al.* (1997a), the apparent better fit between model waves and observations can be partly explained by the presence of swell in most wave systems. Swell is by definition composed of waves which were generated elsewhere and thus earlier in the forecast with winds of better quality or which amplitudes were corrected by previous analyses. Nevertheless, it is also known that the quality of the wave spectrum still under the direct influence of the wind (wind sea component) is intrinsically linked to the quality of the forcing winds (*Janssen et al.* 1997a, *Janssen* 1998, 2000). It is therefore not surprising that the ECMWF wave forecasts are in better agreement with the buoy observations since it appears to be so for the wind speed.

This global picture of the performance of each system should be complemented with the seasonal variation of the different statistics. The time series of the 3 month running average of the analysis and day 3 forecast wave height bias and scatter index are presented in figure 4 for ECMWF, UKMO, FNMOC. The plots clearly illustrate the seasonal variation of the error, as well as the seasonal rate of degradation of the forecasts. By comparing the analysis time series with its forecast counterpart, it also appears that the ECMWF random forecast error has on average a slower growth than the other centre. Over this 3 year period, the characteristics of ECMWF forecast systematic error (bias) has gradually become more similar to the analysis than other centres, indicating that the ECMWF analysis and forecast system has slowly become more consistent.

A comparable analysis can be done for the monthly evolution of the 10m wind speed bias and scatter index. Note however, that the wind observations are included in the data presented to the atmospheric model assimilation. It has been recognised that buoy wind measurements are made by anemometers which are not necessarily located at 10m above mean sea level. Some observations are crudely corrected for this height discrepancy, but most of them are not. In most assimilation systems, no height correction is made to the buoy winds. A general rule is however to multiply the buoy observation by a factor of 1.07 to adjust it to 10 m for neutrally stable atmosphere (*Smith* 1988). Since the atmosphere is not necessarily stable over the areas covered by the buoy networks, implying a different wind profile then neutrally stable, this adjustment would also have errors (*Zambresky* 1989). Without any correction a good analysis fit to the wind might actually result in an underestimation of the real 10 m wind since most buoy anemometer heights are around 5 m potentially resulting in an underestimation of the wave energy generated by the local winds. For example, if the wind speeds were adjusted to 10 m for neutrally stable atmosphere as it is done to produce figure 4, the wind speed bias would be reduced by about 0.5 m/s for a buoy mean wind of 8 m/s. A mean wind speed of 8 m/s with a negative bias of -0.5 m/s can result in a negative wave height bias of -0.2 m (see section 4).

Buoy measurements of the period at the peak of the one dimensional wave spectrum (peak period) are harder to compare to model estimates because of the different methods used to determine it. For example the UKMO model has only 13 frequency components, and the method for calculating the peak period is simply to choose the component with maximum energy. In contrast, the FNMOC model fits a spline to the spectrum before calculating the peak period. The other models are also limited by their frequency resolution (25 bins). For example, the scatter diagrams for analysed peak periods from ECMWF, FNMOC, UKMO are presented in figure 5 for the same collocation as in figure 2. Note however, that this comparison excludes the north east

Atlantic buoys since their GTS records for wave period do not use a peak period definition but rather an integrated weighted spectral mean. A global inspection of these scatter diagrams already indicates the model tendency to overestimate the peak period (see table 6), especially for UKMO. Furthermore, it appears that low buoy values are overestimated but large peak periods are underpredicted.

4.2 Categorised global statistics

Another insight into the data can be obtained by looking at the statistics in function of the observed quantity. In figure 6, the statistics were produced for all sets of model-buoy collocations with buoy data within certain bins. Note that in order to smooth out the plots, the bins overlap. The data used are the same as in previous figures. The evolution of the wave height biases for the analysis and day 2 forecast indicates an slight overestimation for low wave heights and an increasing underestimation for higher wave heights for both ECMWF and FNMOC. Note that this approach might enhance the overestimation of low modelled values because of the positive nature of the studied variables. On the other hand, UKMO wave height bias evolution is quite different with a positive forecast bias for most of the wave height range except for the very high values and a slightly negative bias for the UKMO analysis except for low values. In term of relative random errors (scatter index), the ECMWF wave height analysis and forecasts have the lowest values over the whole observed wave height range.

The analysed wind speed biases for ECMWF and FNMOC are negative for most of the observed wind range except for wind speeds below 4-5 m/s. Meanwhile, UKMO analysis bias is quite small for most of the observed range but increases for high winds. As far as the day 2 forecast is concerned, all centres overestimate low wind speeds. For higher values, FNMOC has a negative bias which can be quite substantial for high wind speeds. Similarly for ECMWF even though the high wind speed bias is less pronounced. Meanwhile, UKMO has a small positive bias. The analysed wind speed scatter index is fairly identical for all 3 centres, whereas the day 2 forecast scatter index favours ECMWF for the full observed range.

The wave peak period can be used to point out which wave system is dominant. When compared to buoy peak periods, all centres have a tendency to predict dominant wave systems with larger peak period until about 11-13 seconds (the wind sea range). In contrast, lower frequency systems (swell) are predicted with a lower peak period. Note that the noticeable difference between UKMO and the other centres should in part be attributed to the cruder method with which UKMO peak periods are determined. The general tendency is nevertheless the same.

4.3 Regional statistics, analysis of the AES system

All statistics presented so far were for all buoys combined, the same can be done by selecting a subset of buoys which are in a region with similar climatological conditions (Figure 1). There are quite some regional differences in analysis and forecast performance. As mentioned in the description of the AES model, wind input to the WAM comes from different CMC atmospheric models. The effects of some of the changes to the wind input are clearly visible in the statistics when they are split between the north Pacific and the north Atlantic regions (Figure 7). The statistics obtained from other centres can be used as references to what could be expected. The GEM model replaced the RFE model in February 1997 without a spin-up cycle and its grid resolution increased to 0.22^{o} in October 1998. These changes seem to have had very little impact on the wave height bias since the model physics and grid resolution were very similar to those of the RFE model. The

impact on the bias following the implementation of the spin-up cycle of the regional GEM model in September 1997 is much more obvious. In the Pacific however, the mainly positive wave height bias gave way to negative bias after implementation of the global GEM model in October 1998. This underprediction is more consistent with the underprediction produced by the wind input from the regional GEM in the Atlantic. The statistics for the east coast are quite different than from the west coast. This feature is not limited to AES, in fact all centres show similar characteristics. It is clear that even though the standard deviation of error is less for the Atlantic buoys, wave heights are generally lower resulting in a larger relative error. Furthermore, intense fast moving disturbances are frequent along the eastern sea shores (cold air outbreaks, coastal jet intensification, rapid cyclogenesis,...). The effects of these systems are harder to model than well developed mid-latitude storms which regularly batter the west coast. Finally, there are always the occasional tropical storms and hurricanes which affects the east coast. The large wave height scatter index at the end of the summer periods (August-September) is attributable to some degree to these intense storms.

In general, both SEF and GEM models have relatively small wind speed biases in both ocean basins. The extremely large bias (~2 m/s) in the spring of 1997 was due to the absence of a spin-up cycle of the regional GEM model as this bias was considerably reduced in the day 2 forecast. In terms of the wind speed scatter index, the same discussion as for the wave height scatter index applies when comparing the Atlantic with the Pacific buoy regions.

4.4 Regional winter and summer statistics

It is also interesting to compile regionally the other model analyses and forecasts for all winter months (December to February) and all summer months (June to August). Figure 8 displays the winter and summer months bias and scatter index evolution for buoys located around the Hawaiian islands. This area is generally dominated by swell and steady winds. These characteristics might explain the relatively slower and uniform wave height error growth compared to other areas (see below).The wind speed bias evolution is quite flat beside the adjustment in the first day (spin up) which might be attributed to some unbalanced physics. The wind speed error growth also shows that ECMWF might not have the best analysis at those locations but it does confirm the quality of its forecasts. As mentioned earlier, a direct comparison of the peak period between the different models is not possible. Nevertheless, a comparison between the summer and winter months indicates that for each centre the relative errors and bias are larger in the summer, even though the wave height errors are lower then. Inspection of time series for buoys around Hawaii (Figure 9) confirms the global statistics.

Swell contribution to the wave field in the north Pacific and along the west coast of north America is also important, however waves are also generated by passing mid latitude storms. Figure 10 illustrates the kind of error which exists for buoys in the north Pacific region. Winter and summer periods exhibit similar relative errors for wind speeds and wave heights. In term of bias, winter periods are characterised by negative analysis biases for wave heights for all WAM models and no bias for UKMO. ECMWF has the largest negative biases. These negative biases can be connected to underestimation of some of the peaks in the wave height time series as illustrated in figure 11. UKMO has no winter bias but tends to overestimate some of the events. Peak period statistics in the winter are better than in the summer as it was the case for Hawaii.

Wave climate along the US and Canadian east coasts is less influenced by long swell which have propagated from far, except in the summer when local winds are weak. These areas are however subject to rapidly

developing storms and frontal passages which are usually intensifying during the transition from land to sea. It is also on the tracks of occasional hurricanes. Under these conditions, it is not surprising that it is a more difficult area for wave modelling. Figure 12 displays the type of statistics which can be obtained from the comparison with the selected buoys along the US east coast. By comparing it with statistics from buoys on the other side of the north American continent (figure 10) or on the other side of the Atlantic (figure 14), it is clear that in relative terms, the errors are larger. A similar conclusion can also be made for the Japanese buoys (not shown). ECMWF which has a clear advantage for any other regions, has comparable scatter index for its analysis and short range forecasts than the other centres, yet with a larger negative bias in the winter. Figure 13 is an example of wind and wave analyses for buoys along the US east coast.

Finally, statistics for buoys on the Atlantic front of the British Isles are displayed in figure 14. In terms of scatter index, this region is well modelled. ECMWF and FNMOC have a tendency to underestimate maxima in the wave height time series, resulting in a systematic negative bias, while UKMO can have it both ways as shown in figure 15.

5. Discussion and implications for ECMWF

It is beyond the scope of this paper to review all the different aspects of each system in order to understand the observed differences. In the 3 years covered by this study, both atmospheric and wave models have gone through a series of changes, while some characteristics of each model have remained. UKMO is still using a second generation wave model with limited frequency and angular resolution. A comparison between second and third generation wave models has already been extensively covered in the past (*SWAMP* 1985, *SWIM* 1985) and even more recently by *Fradon et al.* 2000.

Even with the same original model (WAM), large differences still exist. The quality of the wind forcing is essential for the good performance of the wave model. It also determines to a large extend the evolution of the forecast errors (*Janssen* 1998). Nevertheless some aspects of the respective implementation of WAM can be discussed considering that differences already exists for analyses.

The benefit of assimilating altimeter wave height (ECMWF, UKMO, NCEP) has been re-evaluated by running a version of the ECMWF global wave model in an uncoupled mode with 6 hourly analysed winds with or without satellite data for February and July 1999. The comparison with the buoy data indicated a net decrease in both systematic and random error (table 7), confirming the advantage of such schemes.

It is known that wave spectral directional spreads have a tendency to be too broad, partly due to the limited number of directional bins used by the numerical models. An increase in angular resolution also has a positive impact on the quality of the modelled waves. Table 8 displays the statistics for February 1999 of uncoupled analysis runs with the ECMWF model with respectively 12, 18, 24 directions. No altimeter data were used. Doubling the angular resolution does improve the wave model performance.

Following this recommendation, ECMWF increased its angular resolution from 12 to 24 in November 2000. It does appear that FNMOC should make use of the altimeter data, especially since in the future more near real time altimeter data will become available (Envisat, Jason,...)

The buoy wind speed observations are included in the data used by the atmospheric data assimilation. However, those observations are generally assumed to be 10m wind speeds and are thus assimilated without any height correction. Figure 1 shows that most buoys carry an anemometer at around 5m. All wind speed statistics presented so far were obtained by correcting the observed wind speeds using a logarithmic wind profile. A similar compilation can be done without any correction (as was done before). For instance figure 16 presents the difference between the binned bias statistics for observed wind speeds and their corrected counterparts (as in figure 6) for all buoys. Also shown are the differences between neutral winds at 5 or 7.5m and the corresponding values at 10m. These differences can be interpreted as the maximum systematic bias that might be introduced by the analysis system when it tries to fit the model to the uncorrected wind observations. This problem might even get worse when the analysis scheme is tailored to take into account hourly wind observations as it is the case in the ECMWF 4dvar scheme. Although, this systematic bias may seem quite small, it may still result in a considerable bias in wave height. Starting from the equilibrium relation between wave height H_s and wind speed U_{10} (*Komen at al.* 1994).

$$H_s = \beta U_{10}^2 / g \tag{1}$$

where g is the acceleration of gravity, and β is in general a function of U_{10}, but in first approximation it can be taken to be a constant (0.22) (*Janssen et al.* 1997a), the wave height bias (δHs) caused by a systematic wind bias (δU_{10}) can be estimated by

$$\delta Hs = (2\beta U_{10} \delta U_{10}) / g \tag{2}$$

This estimate is also plotted in figure 16 for each wind speed bias. For large wind speeds, the maximum wave height underestimation could be as large as 1m. In section 4, we have also shown that analysed wave heights for all WAM model configurations were sometimes significantly underestimated in the peaks of the time series. It is therefore reasonable to argue that some of this underestimation when linked to local wave growth might in part be explained by this systematic negative bias in analysed wind speed. Moreover, looking back at the evolution of the forecast wind speed errors (fig. 8,10,12,14), it appears as if the analysis systematic error behave some what differently than the forecast biases (mostly for ECMWF).

Results from figure 16 can be used to estimate what effect this analysis bias might have on the wave statistics. Table 9 presents analysed wave height statistics for the same buoy data as table 2 but with model wave heights corrected with the relationship derived from all wind speed data (the curve with the triangles). Not surprisingly, all WAM model systems which do not use buoy wave heights in their analysis have better statistics. The present discussion does not really apply to UKMO. As found in figure 6, and by looking at the wind speed time series, UKMO wind speed analysis has a tendency to exaggerate some of the high wind events resulting in overpredicted wave heights.

In view of these results, there is no doubt that the actual anemometer height should be used to correct buoy wind speed observations. ECMWF has actually developed a corrective scheme for buoy and ship observations. It relies on a list of proper anemometer height which was put together by gathering informations on ships and buoys. It uses the actual ocean boundary layer physics to adjust the observation to 10m (Drasko Vasiljevic personal communication). The scheme has been in place since July 1999 (cycle CY21R2), however, all buoys used in this study were missing from the list until February 2000. Furthermore, a bug in the procedure prevented its application (for buoys) until the operational introduction of cycle 22R3 (June 27,

2000). A short experiment (9 days) does however show the benefit of the corrective scheme (table 10). The impact of this scheme is not as large as could be expected from figure 16, however ship and buoy observations are usually not the only source of information in the vicinity of the buoys. Note also that buoy and ship wind speed data contain inherent truncation errors of +- 0.5 m/s. Finally the 4dvar analysis error estimate of ship and buoy data might still too large for those moored buoys equipped with high quality anemometer. It is hoped that in the future the actual anemometer height will be included in the buoy data record and whether or not the wind observation were adjusted to 10m. It will remove the need for a continual updating of a corrective list. Similarly, a higher precision of the reported wind measurements is desired if one wants to fully profit from these observations in a data assimilation of ever increasing complexity.

In an attempt to understand the different quality level of the ECMWF wind and wave analysis between buoys along the west and the east coast of the US and Hawaii, a Fourier analysis of the wind speed hourly time series for a few buoys from the American network was performed. Instead of using GTS data, data from the NOAA Marine Environmental Buoy Database were obtained (http://www.nodc.noaa.gov/) in order to get quality controlled wind speed data with a higher precision (rounded to the closest 0.1 m/s) than the GTS raw data. These observations were blended with hourly model data obtained from the analysis feedback files which already contain hourly collocations between GTS and model first guess and analysis data as well as the quality flags used by the analysis system. Buoys with very few missing records and analysis rejections for the period of October 1999 to February 2000 were selected. Observed wind speed were adjusted to 10m using the same procedure as for GTS data. The respective frequency spectra of the observed, first guess and analysed 10m wind speed are presented in figures 17 to19. On these log-log plots, linear fits for the mean slope in the interval 100 to 10 hours are also displayed in an attempt to show how the model first guess and analysis represent the different scales of variability. For buoys located along the western US (figure 17), there is a fairly good agreement at all scales between model and observations. The situation deteriorates slightly for buoys along the eastern US and the Gulf of Mexico (figure 18) with a larger discrepancy at shorter scales. The lack of short scale representation can only be detrimental to the wave growth process (*Komen et al.* 1994) which was found to be particularly insufficient in that region (figures 12-13). The wind speed spectra for Hawaii indicate that first guess and analysis agree less with each other than for other locations (figure 19). Furthermore, short scales in neither model estimates correspond to the observed ones. The effect on the waves of such disparity is less clear. As noted in figure 8, Hawaiian buoys are dominated by swell, nevertheless, the effect of the local wind should not be ignored. Part of the wave height negative bias could well be attributed to this lack of short scales representation. Moreover, the reduced variability in the modelled winds may have a detrimental impact on peak period statistics near Hawaii, because wind seas are presumably underestimated.

6. Conclusions

Every month, wave model analysis and forecasts from five participating centres are compared with buoy observations at selected locations. The buoy data are obtained from the GTS and a basic quality control and averaging is used to produce observed data which can be compared to the equivalent model values. The resulting statistics serves as an additional validation tool for the operational wave forecasting system of each collaborating centre (winds and waves). The comparison provides an independent reference for operational changes or problems which could otherwise go unnoticed.

This information can be used to identify wind and wave modelling shortcomings. It was shown that all global implementations of the third generation wave model WAM have a tendency to underpredict wave height when forced by analysed wind fields. On the other hand, it appears that beside using a different wave model, UKMO system tends to have 10m winds which are overestimated. The resulting wave analysis and forecasts in the areas where wave generation is important is therefore in the mean less underestimated, however, overpredictions occur more often. As a whole, the ECMWF system seems to perform the best, there are however regional differences. ECMWF appears to have more difficulties in representing wind and wave conditions on the western side of the ocean basins (US east coast and Japan). The comparison of the forecasting system at four of the five participating centres using the same original wave model (WAM) has also shown the essential importance of good quality winds. The centre with the best forecast winds (ECMWF) also has the best wave forecasts. It is however noted that the qualitative assessment of the forcing winds might require more than just a study of basic statistics such as bias and rmse. A short analysis of the different scales present in the observed and model winds reveals that model wind might under represents some of the shortest scales.

Looking back at some of the differences in the implementation of WAM indicates the positive impact of assimilating altimeter wave heights (as suggested to FNMOC). It also illustrates the benefit of an increase in angular resolution of the discretised wave spectrum (as done at ECMWF).

Due to the design of the meteorological buoys, wave but also wind data are reported. It was argued that since buoy winds are not corrected for the actual height of the anemometers, a systematic bias might be present in the wind analysis which in turn could explained some of the analysed wave height underestimations. Effort should be made to adjust the wind data before they can be used by the model assimilation as it is now possible at ECMWF.

It is believed that centres engaged in wave forecasting will benefit from this activity in the same way as weather centres benefit from the exchange of forecast verification scores. Everyone involved in the project knows the actual skill of the model forecasts, and sees what kind of errors should be tackled first. Ultimately it could lead to improvements of future wave models.

Finally, it is hoped that by making the information widely available, it will stimulate a more comprehensive exchange of wave data with organisations which collect wave data but do not make them available on GTS.

ACKNOWLEGMENTS

Careful reading and constructive comments by Peter Janssen and Martin Miller are gratefully acknowledged. We also want to thank the NOAA National Oceanographic Data Center for their on-line access to buoy data. We would like to thank Els Kooij-Connally and Rob Hine for their help in editing this document.

6. References

Bauer E., C. Staabs, 1998: Statistical properties of global significant wave height and their use for validation, *J. Geophys. Res.*, **103C**, 1153-1166.

Bengston L., 1999: From short-range barotropic modelling to extended-range global weather prediction: a 40 year perspective. *Tellus*, **51** A-B, 13-32.

Bidlot J.-R., P. Janssen, B. Hansen and H. Günther, 1997: A modified set up of the advection scheme in the ECMWF wave model. *ECMWF Tech. Memo. 237*, ECMWF, Reading, United Kingdom, 31pp.

Bidlot J.-R., M. Holt, P. A. Wittmann, R. Lalbeharry, H. S. Chen, 1998: Towards a systematic verification of operational wave models. *Proc. Third Int. Symposium on WAVES97:* November 3-7, 1997, Virginia Beach, Va, USA, edited by B. L. Edge and J. M. Hemsley. American Society of Civil Engineer.

Bidlot J.-R., M. Holt, 1999: Numerical wave modelling at operational weather centres. *Coastal Engineering,* **37**, 409-429.

Buckley A. L 1999: Wave Current Interaction for the Met Office Wave Model. *Met Office (Ocean Applications) Internal Paper* No. 22

Buizza R., A. Hollingsworth, A. Lalaurette and A. Ghelli, 1999: Probabilistic prediction of precipitation using the ECMWF ensemble prediction system. *Weather and Forecasting*, **14**, 168-189.

Cardone, V. J., 1987: The present status of operational wave forecasting. *John Hopkins APL Tech. Dig.*, **8**, 24-32.

Charnock H., 1955: Wind stress on a water surface. *Quart. J. Roy. Meteor. Soc.*, **81**, 639-640.

Chen H.S. 1995: Ocean surface waves. TPB 426, NOAA/NWS/OM, 18pp.

Chouinard C., J. Mailhot, H.L. Mitchell, A. Staniforth and R. Hogue, 1994: The Canadian data assimilation system: Operational and research applications. *Mon. Wea. Rev.*, **122**, 1306-1325.

Clancy, R. M., J. E. Kaitala, and L.F. Zambresky, 1986: The Fleet Numerical Oceanography Centre Global Spectral Ocean Wave Model. *Bull. Amer. Meteor. Soc.*, **67**, 498-512.

Côté J., S. Gravel, A. Methot, A. Patoine, M. Roch and A. Staniforth, 1998a: The operational CMC/MRB Global Environmental Multi-scale (GEM) model: Part I - Design considerations and formulation. *Mon. Wea. Rev.*, **126**, 1373-1395.

Côté J., J.G. Desmarais, S. Gravel, A. Methot, A. Patoine, M. Roch and A. Staniforth, 1998b: The operational CMC/MRB Global Environmental Multi-scale (GEM) model: Part II - Results. *Mon. Wea. Rev.*, **126**, 1397-1418.

Delage Y., 1997: Parameterizing sub-grid scale vertical transport in atmospheric models under statistically stable conditions. *Boundary-Layer Meteorol.*, **82**, 23-48.

Delage Y. and C. Girard, 1992: Stability functions correct at the free convection limit and consistent for both the surface and Ekman layers. *Boundary-Layer Meteorol.*, **58**, 19-31.

Derber J. and F. Bouttier, 1999: A reformulation of the background error covariance in the ECMWF global data assimilation system. *Tellus*, **51A**, 195-221.

Foreman S.J., M.W. Holt, and S. Kelsall 1994: Preliminary assessment and use of ERS-1 altimeter data. *J. Atmos. Oceanic Technol.*, **13**, 1370-1380.

Fradon B., D. Hauser, and J.-M. Lefevre, 2000: Comparison study of a second generation and of a third generation wave prediction model in the context of the semaphore experiment. *J. Atmos. Oceanic Technol.*, **17**, 197-214.

Gauthier, P., C. Charette, L. Fillion, P. Koclas and S. Laroche, 1999: Implementation of a 3D variational data assimilation system at the Canadian Meteorological Centre. Part I: The global analysis. *Atmosphere-Ocean*, **37**, 103-156.

Golding B. 1983: A wave prediction system for real time sea state forecasting', *Quart. J. R. Met. Soc.*, **109**, 393-416.

Hoffschildt M., J.-R. Bidlot, B. Hansen, P.A.E.M. Janssen, 1999: Potential benefit of ensemble forecasts for ship routing. *ECMWF Technical Memorandum* No. 287. ECMWF Reading, United Kingdom, 25pp.

Hodur, R.M., 1997: The Naval Research Laboratory's Coupled Ocean/Atmosphere Mesoscale Prediction System (COAMPS). *Mon. Wea. Rev.*, **125**, 1414-1430

Hogan, T.F, and T.E Rosmond, 1991: The Description of the U.S. Navy Operational Global Atmospheric Prediction System's Spectral Forecast Model. *Mon. Wea. Rev.*, **119**, 1786-1815.

Holt M.W. 1994: Improvement to the UKMO wave model swell dissipation and performance in light winds, *Met. Office Forecasting Research Division Technical Report* No.119 (unpublished document, copies available from national meteorological library).

Holt M.W. 1997:Assimilation of ERS-2 altimeter observations into a global wave model, *WGNE: Research activities in atmospheric ans oceanic modelling,* 1997, 8.31-8.32.

Janssen P.A.E.M., 1989: Wave-induced stress and the drag of air flow over sea. *J. Phys. Oceanogr.*, **19**, 745-754.

Janssen P.A.E.M., 1991: Quasi-linear theory of wind wave generation applied to wave forecasting. *J. Phys. Oceanogr.*, **19**, 1631-1642.

Janssen P.A.E.M., 1998: On error growth in wave models. *ECMWF Technical Memorandum*, No.249, ECMWF Reading, United Kingdom, 12pp.

Janssen P., 1999: Wave modeling and altimeter wave height data, *ECMWF Technical Memorandum*, No.269. ECMWF Reading, United Kingdom, 35pp.

Janssen P., 2000: Wave modeling and altimeter wave height data. In *Satellite, Oceanography and Society*, 35-56, edited by D. Halpern, Elsevier Science.

Janssen P.A.E.M. and P. Viterbo, 1996: Ocean wave and the atmospheric climate. *J. Climate,* **9**, 1269-1287.

Janssen P.A.E.M., B. Hansen, J.-R. Bidlot 1997a: Verification of the ECMWF wave forecasting system against buoy and altimeter data. *Weather and Forecasting*, **12**, 763-784.

Janssen P.A.E.M., J. D. Doyle, J. Bidlot, B. Hansen, L. Isaksen and P. Viterbo, 2000a: Impact of ocean waves on the atmosphere. *Seminar on atmosphere-surface interaction*, 8-12 September 1997 at ECMWF, 85-111. ECMWF, Reading, UK.

Janssen P.A.E.M, J.-R. Bidlot, and B. Hansen, 2000b: Diagnosis of ocean-wave forecasting systems. *Seminar on diagnostics of models and data assimilation systems,* 6-10 September 1999 at ECMWF, 233-256. ECMWF, Reading, UK.

Khandekar, M. L., and R. Lalbeharry, 1996: An evaluation of Environment Canada's operational wave model based on moored buoy data. *Wea. Forecasting*, **11**, 139-152.

Komen G.J., L. Cavaleri, M. Donelan, K. Hasselmann, S. Hasselmann and P.A.E.M. Janssen, 1994: Dynamic and Modelling of ocean waves, Cambridge University Press.

Laroche, S., P. Gauthier, J. St-James and J. Morneau, 1999: Implementation of a 3D variational data assimilation system at the Canadian Meteorological Centre. Part II: The regional analysis. A*tmosphere-Ocean*, **37**, 281-307.

Lionello P., H. Günther and P.A.E.M Janssen, 1992: Assimilation of altimeter data in a global third generation wave model. *J. Geophys. Res.,* **C97**, 14453-14474.

Mahfouf J.F., F. Rabier, 2000: The ECMWF operational implementation of four dimensional variational assimilation. Part II: Experimental results with improved physics. *Quart. J. Roy. Meteor. Soc.126,* **126**, 1171-1190

Mailhot J., R. Sarrazin, B. Bilodeau, N. Brunet, A. Methot, G. Pellerin, C. Chouinard, L. Garand, C. Girard and R. Hogue, 1995: Changes to the Canadian regional forecast system: Description and evaluation of the 50-km version. *Atmosphere-Ocean,* **33**, 55-80.

Mailhot J., R. Sarrazin, B. Bilodeau, N. Brunet and G. Pellerin, 1997: Development of the 35km version of the Canadian regional forecast system. *Atmosphere-Ocean*, **35**, 1-28.

Monaldo F., 1988: Expected difference between buoy and radar altimeter estimates of wind speed and significant wave height and their implications on buoy-altimeter comparisons, *J. Geophys. Res.*, **93C**, 2285-2302.

Rabier. F., H. Jarvinen, E. Klinker, J.F. Mahfouf, and A. Simmons, 2000: The ECMWF operational implementation of four dimensional variational assimilation. Part I: Experimental results with simplified physics. *Quart. J. Roy. Meteor. Soc.*, **126**, 1143-1170.

Ritchie H. and C. Beaudoin, 1994: Approximations and sensitivity experiments with a baroclinic spectral model. *Mon. Wea. Rev.*, **122**, 2391-2399.

Romeiser, R., 1993: Global validation of wave model WAM over a one year period using Geosat wave height data. *J. Geophys. Res.*, **98C**, 14453-14474.

Smith S., 1988: Coefficients for sea surface wind stress, heat flux and wind profiles as a function of wind speed and temperature. *J. Geophys. Res.*, **93C**, 15467-15472.

Steenbergen, D., A. Simard and P. Dubreuil, 1998: Towards operational 10 km forecasts at the Canadian Meteorological Centre (CMC). *CMOS Bulletin*, **26**, 41-43.

Sterl, A. G., G. J. Komen, and P. D. Cotton, 1998: Fifteen years of global wave hindcasts using ERA winds: Validating the reanalysed winds and assessing the wave climate, *J. Geophys. Res.*, **103C**, 5477-5492.

SWAMP Group, 1985: Sea Wave Modelling Project (SWAMP). An intercomparison study of wind wave prediction models, Part 1: Principal results and conclusions. *Ocean Wave Modelling*, Plenum Press, New York, 3-153.

SWIM Group, 1985: Shallow water intercomparison of wave prediction models (SWIM). *Quart. J. Roy. Meteor. Soc.*, **111**, 1087-1113.

Thomas J. P., 1988: Retrieval of energy spectra from measured data for assimilation into a wave model. *Quart. J. Roy. Met. Soc.*, **114**, pp.781-800.

Tolman H.L., 1999: User manual and system documentation of WAVEWATCH-III version 1.18. *NOAA/NWS OMB Contribution* no. 166. 110pp.

Wittmann, P. A., R. M. Clancy, and T. Mettlach, 1995: Operational wave forecasting at Fleet Numerical Meteorology and Oceanography Center, Monterey, CA. *Fourth Int. Workshop on Wave Hindcasting and Forecasting,* Banff, AB, Canada, Atmospheric Environment Service, 335-342.

Wittmann, P. A. and R.M. Clancy, 1994: Implementation and validation of a global third-generation wave model. In *Ocean Wave Measurement and Analysis*, Proceeding of the Second International Symposium, 25-28 July 1993, New Orleans, O.T. Magoon and J.M. Hemsley, Editors, American Society of Civil Engineers, 345 East 47th Street, New York, NY 10007-2398, pp. 406-419.

Wittmann, P. A. and T.C Pham, 1999: Coastal Wave Predictions Forced by Mesoscale Winds. *Third Conference on Coastal Atmospheric and Oceanic Prediction Processes.* New Orleans, LA. 3-5 Nov., 1999, 113-115

Zambresky L., 1987: The operational performance of the Fleet Numerical Oceanography Center global spectral ocean-wave model. *John Hopkins APL Tech. Dig.*, **8**, 33-36.

Zambresky L., 1989: A verification study of the global WAM model. December 1987-November 1988. *ECMWF Technical Report* No.63, ECMWF, Reading, United Kingdom, 86pp.

Tables

	E.C.M.W.F	U.K.M.O	F.N.M.O.C	A.E.S	N.C.E.P
MODEL	WAM 4.0	2nd generation	WAM 4.0	WAM 4.0	WAM 4.0
DOMAIN	global	global	global	Atl. & Pac. North of 25°N	global
GRID	55 km x 55 km	0.833°x1.25° *	1.0°x1.0°	1.0°x1.0°	2.5°x2.5°
Spectral Discretisation	25 frequencies 12 directions	13 frequencies 16 directions	25 frequencies 24 directions	25 frequencies 24 directions	25 frequencies 12 directions
wave physics	shallow water	deep water **	deep water	deep water	deep water
WIND	coupled to T319 10 m winds	lowest sigma level NWP model	Wind stress T159 NOGAPS	GEM 10m winds Atl. regional & Pac. global mod.	lowest sigma level corrected to 10m
WIND INPUT	hourly	hourly	3 hourly	3 hourly	3 hourly
Altimeter data	yes	yes	no	no	yes ***
Ice edge	yes	yes	yes	yes	yes
Start of forecast	0 and 12Z	0 and 12Z	0 and 12Z	0 and 12Z	0 and 12Z
Forecast range	10 days	5 days	6 days	2 days	3 days

Table 1: Wave model description

* In May 1999, increase in resolution to 60km at mid latitude.

** In May 1999, shallow water.

*** Assimilate buoy data as well since February 1998.

t + 0	ECMWF	UKMO	FNMOC	AES	NCEP
Number of entries	25343	25343	25343	12528	17788
Buoy mean (m)	2.49	2.49	2.49	2.55	2.53
Bias (m)	-0.17	0.04	-0.06	-0.13	0.03
R.M.S.E. (m)	0.46	0.52	0.49	0.55	0.43
Scatter index	0.17	0.21	0.20	0.21	0.17
Symmetric slope	0.91	1.01	0.95	0.97	1.00

Table 2: Analysed wave height statistics from December 1996 to December 1999. Negative bias denotes lower model values with respect to buoy observations. The scatter index is defined as the standard deviation of the difference between model and buoy normalised by the observation mean. The symmetric slope refers to the ratio of the sum of the squares of the model results with the sum of the squares of the observations.

t + 0	ECMWF	UKMO	FNMOC	AES	NCEP
Number of entries	23820	23820	23820	11342	16747
Buoy mean (m/s)	7.39	7.39	7.39	7.46	7.43
Bias (m/s)	-0.31	0.16	-0.37	0.03	-0.27
R.M.S.E. (m/s)	1.43	1.42	1.43	1.83	1.96
Scatter index	0.18	0.18	0.18	0.23	0.25
Symmetric slope	0.97	1.03	0.96	1.02	0.98

Table 3: Analysed 10m wind speed statistics from December 1996 to December 1999. Negative bias denotes lower model values with respect to buoy observations. The scatter index is defined as the standard deviation of the difference between model and buoy normalised by the observation mean. The symmetric slope refers to the ratio of the sum of the squares of the model results with the sum of the squares of the observations. The buoy wind data were adjusted to neutrally stable 10m wind using a logarithmic vertical profile with a Charnock parameter of 0.018.

t + 2	ECMWF	UKMO	FNMOC	AES	NCEP
Number of entries	25334	25334	25343	12508	18161
Buoy mean (m)	2.49	2.49	2.49	2.55	2.52
Bias (m)	-0.13	0.20	0.03	-0.17	0.24
R.M.S.E. (m)	0.60	0.76	0.65	0.68	0.72
Scatter index	0.23	0.29	0.26	0.26	0.27
Symmetric slope	0.94	1.08	0.99	0.94	1.08

Table 4: Same as table 2 but for the day 2 forecasts started from 12Z analyses.

t + 2	ECMWF	UKMO	FNMOC	AES	NCEP
Number of entries	23746	23746	23746	11290	17290
Buoy mean (m/s)	7.39	7.39	7.39	7.47	7.41
Bias (m/s)	-0.02	0.56	0.09	-0.01	0.12
R.M.S.E. (m/s)	2.37	2.75	2.79	2.78	2.68
Scatter index	0.30	0.34	0.35	0.35	0.34
Symmetric slope	1.00	1.08	1.01	1.00	1.02

Table 5: Same as table 3 but for the day 2 forecasts started from 12Z analyses

t + 0	ECMWF	UKMO	FNMOC
Number of entries	19665	19665	19665
Buoy mean (s)	9.44	9.44	9.44
Bias (s)	0.26	1.57	0.23
R.M.S.E. (s)	2.16	3.54	2.20
Scatter index	0.23	0.34	0.23
Symmetric slope	1.02	1.17	1.04

Table 6: Same as table 2 but for peak periods.

February 1999	Hs no alt	Hs with alt	Tp no alt	Tp with alt
Number of entries	6829	6829	4243	4243
Buoy mean	2.80 m	2.80 m	9.35 s	9.35 s
Bias	-0.38 m	-0.22 m	-0.57 s	-0.08 s
R.M.S.E.	0.64 m	0.52 m	1.89 s	1.76 s
Scatter index	0.18	0.17	0.19	0.19
Symmetric slope	0.87	0.91	0.95	1.00
July 1999	Hs no alt	Hs with alt	Tp no alt	Tp with alt
Number of entries	7486	7486	4525	4525
Buoy mean	1.31 m	1.31 m	7.40 s	7.40 s
Bias	-0.09 m	-0.01 m	0.64 s	1.07 s
R.M.S.E.	0.29 m	0.25 m	2.48 s	2.62 s
Scatter index	0.21	0.19	0.32	0.32
Symmetric slope	0.93	0.97	1.12	1.15

Table 7: Statistics from two runs of one month each of the stand alone 0.5° ECMWF WAM model with or without assimilation of altimeter wave heights. Statistics for wave heights (Hs) are given in the two left columns and those for peak periods (Tp) in the two right columns. All runs were forced by 6 hourly winds from the ECMWF operational analysis.

Hs February 1999	12 directions	18 directions	24 directions
Number of entries	6829	6829	6829
Buoy mean (m)	2.80	2.80	2.80
Bias (m)	-0.42	-0.41	-0.38
R.M.S.E. (m)	0.66	0.65	0.63
Scatter index	0.18	0.18	0.18
Symmetric slope	0.85	0.86	0.87
Tp February 1999			
Number of entries	4243	4243	4243
Buoy mean (s)	9.35	9.35	9.35
Bias (s)	-0.51	-0.50	-0.43
R.M.S.E. (s)	1.88	1.91	1.88
Scatter index	0.19	0.20	0.20
Symmetric slope	0.96	0.96	0.97

Table 8: Statistics from one month runs of the stand alone 0.5° ECMWF WAM model with different angular resolutions for the wave spectra. Statistics for wave heights (Hs) are given in the top panel and those for peak periods (Tp) in the bottom one. All runs were forced by 6 hourly winds from the ECMWF operational analysis and altimeter data were not used.

t + 0	ECMWF	UKMO	FNMOC	AES	NCEP
Number of entries	25342	25342	25342	12528	17787
Buoy mean (m)	2.49	2.49	2.49	2.55	2.53
Bias (m)	0.01	0.22	0.13	0.06	0.21
R.M.S.E. (m)	0.41	0.61	0.49	0.57	0.49
Scatter index	0.16	0.23	0.19	0.22	0.18
Symmetric slope	0.99	1.09	1.03	1.04	1.07

Table 9: Same as in table 2 except that the wave model data were adjusted using the empirical relation derived in figure 16.

WIND end of March 2000	reference	height corrected
Number of entries	1856	1856
Buoy mean (m/s)	7.08	7.08
Bias (m/s)	-0.34	-0.26
R.M.S.E. (m/s)	1.47	1.47
Scatter index	0.20	0.20
Symmetric slope	0.95	0.96
WAVE HEIGHT end of March 2000	reference	height corrected
Number of entries	2076	2076
Buoy mean (m)	2.10	2.10
Bias (m)	-0.22	-0.21
R.M.S.E. (m)	0.45	0.44
Scatter index	0.19	0.18
Symmetric slope	0.90	0.91

Table 10: Buoy statistics for 9 days of the ECMWF coupled analysis system from March 23, 2000 to the end of March 2000. The reference is compared to a run in which wind speed from buoys were adjusted to 10m.

1	21004	JAPAN	7.5m	JMA	Shikoku South	E,U,F,N
2	22001	JAPAN	7.5m	JMA	Ryukyu Islands	E,U,F,N
3	41001	USEC	5.0m	NDBC	East Hatteras	E,U,F,N,A
4	41002	USEC	5.0m	NDBC	South Hatteras	E,U,F,N,A
5	41010	USEC	5.0m	NDBC	Cape Canaveral East	E,A
6	42001	GM	10.0m	NDBC	Mid Gulf of Mexico	E,U,F,N
7	42003	GM	10.0m	NDBC	Eastern Gulf of Mexico	E,U,F,N
8	44004	USEC	5.0m	NDBC	Hotel	E,U,F,N,A
9	44008	USEC	5.0m	NDBC	Nantucket	E,U,F,N,A
10	44011	USEC	5.0m	NDBC	Georges Bank	E,U,F,N,A
11	44137	CANEC	5.0m	CMEDS	East Scotia slope	E,F,A
12	44138	CANEC	5.0m	CMEDS	SW Grand Bank	E,F,N,A
13	44141	CANEC	5.0m	CMEDS	Laurentian Fan	E,F,N,A
14	44142	CANEC	5.0m	CMEDS	Lahave Bank	E,F,N,A
15	46001	NPC	5.0m	NDBC	Gulf of Alaska	E,U,F,N,A
16	46002	USWC	5.0m	NDBC	Oregon	E,U,F,N,A
17	46003	NPC	5.0m	NDBC	Aleutian Peninsula	E,U,F,N,A
18	46004	NPC	5.0m	CMEDS	Middle Nomad	E,U,F,N,A
19	46005	USWC	5.0m	NDBC	Washington	E,U,F,N,A
20	46006	USWC	5.0m	NDBC	SE Papa	E,U,F,N,A
21	46035	NPC	5.0m	NDBC	Bering Sea	E,U,F,N,A
22	46036	USWC	5.0m	CMEDS	South Nomad	E,U,F,N,A
23	46059	USWC	5.0m	NDBC	California	E,F,N,A
24	46184	NPC	5.0m	CMEDS	North Nomad	E,U,F,N,A
25	51001	HW	5.0m	NDBC	Hawaii North West	E,U,F,N
26	51002	HW	5.0m	NDBC	Hawaii South West	E,U,F,N
27	51003	HW	5.0m	NDBC	Hawaii West	E,U,F,N
28	51004	HW	5.0m	NDBC	Hawaii South East	E,U,F,N
29	62029	NEATL	4.5m	UKMO	K1	E,U,F,N
30	62081	NEATL	4.5m	UKMO	K2	E,U,F,N
31	62105	NEATL	4.5m	UKMO	K4	E,U,F,N
32	62106	NEATL	4.5m	UKMO	RARH	E,F
33	62108	NEATL	4.5m	UKMO	K3	E,U,F,N
34	62163	NEATL	4.5m	UKMO	Britanny	E,F,N
35	63111	NSEA	10.0m	UKMO	Platform Beryl	E,U,F,N
36	64045	NEATL	4.5m	UKMO	K5	E,F,N

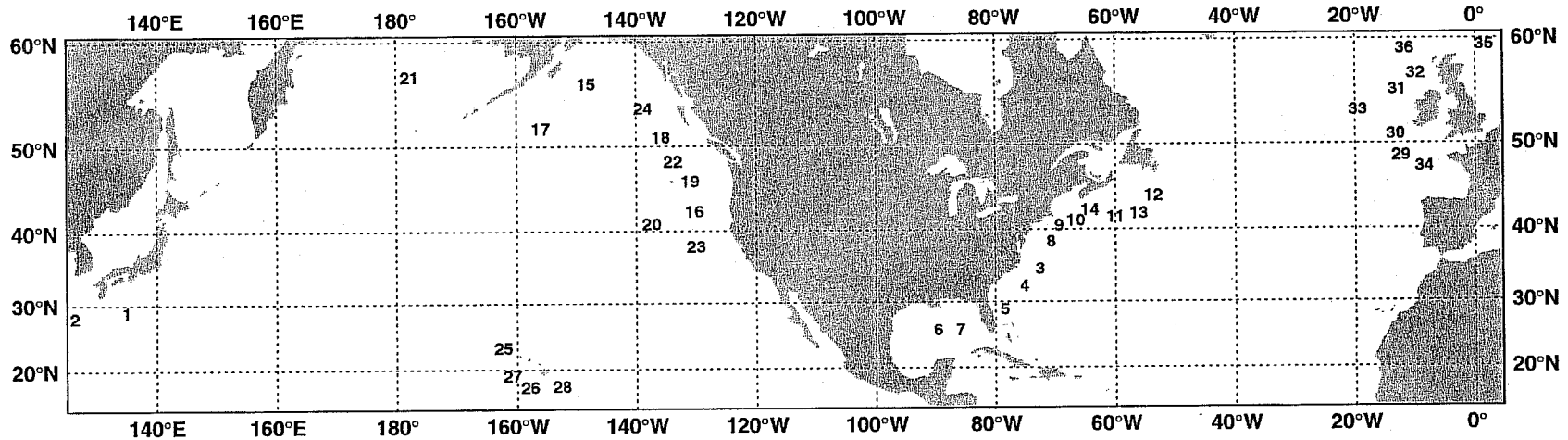

Figure 1: Locations of all buoys used in the comparison. In the accompanying table, the 5 digit WMO buoy identifier is followed by the abbreviated name of the region to which it belongs when compiling statistics per area: Hawaii (HW), Japan (JAPAN), the North Pacific (NPC), US West Coast (USWC), US East Coast (USEC), Gulf of Mexico (GM), Canadian East Coast (CANEC), The North East Atlantic (NEATL), and the North Sea (NSEA). It is followed by the actual height of the anemometer as was obtained from the different data provider: the Japanese Meteorological Agency (JMA), the National Data Buoy Center (NDBC), the Canadian Marine Environmental Data Service (CMEDS) and the United Kingdom Meteorological Office (UKMO). When known, the name used by the data provider or the geographical location is shown along with the first initial of each centre for which model data are also available.

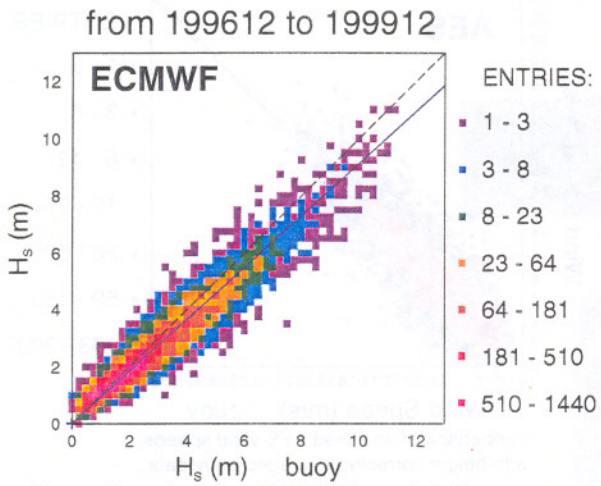

Comparison of analysed ECMWF wave heights with averaged buoy data.

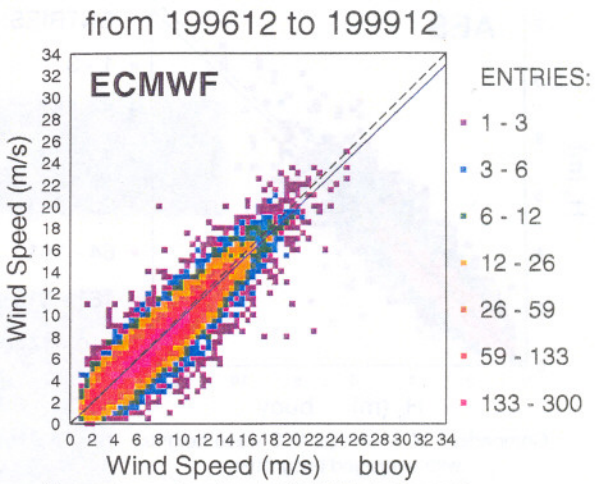

Comparison of analysed ECMWF wind speeds with height corrected averaged buoy data.

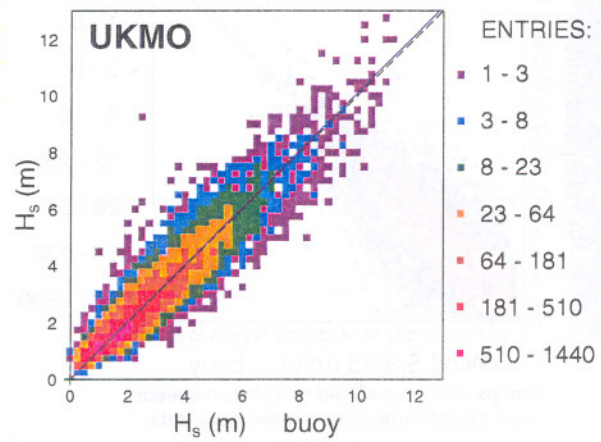

Comparison of analysed UKMO wave heights with averaged buoy data

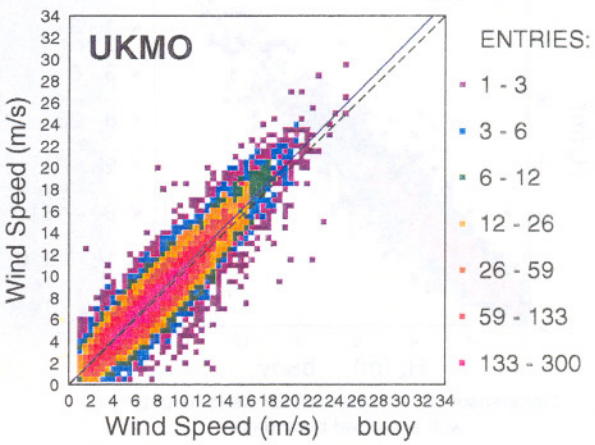

Comparison of analysed UKMO wind speeds with height corrected averaged buoy data.

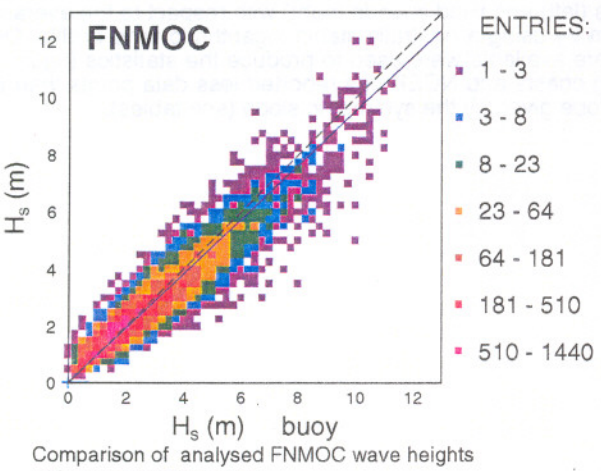

Comparison of analysed FNMOC wave heights with averaged buoy data.

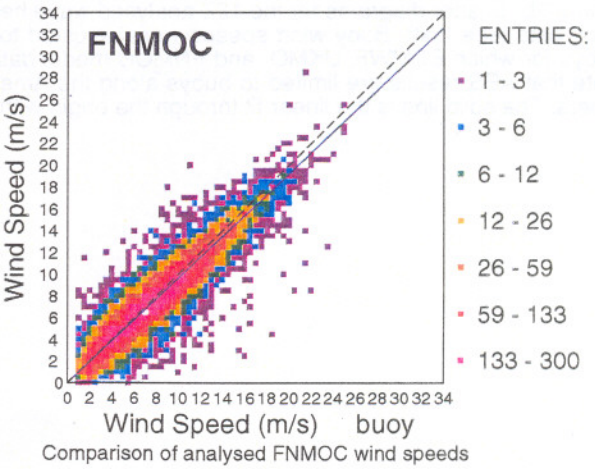

Comparison of analysed FNMOC wind speeds with height corrected averaged buoy data.

Figure 2a: see figure 2b

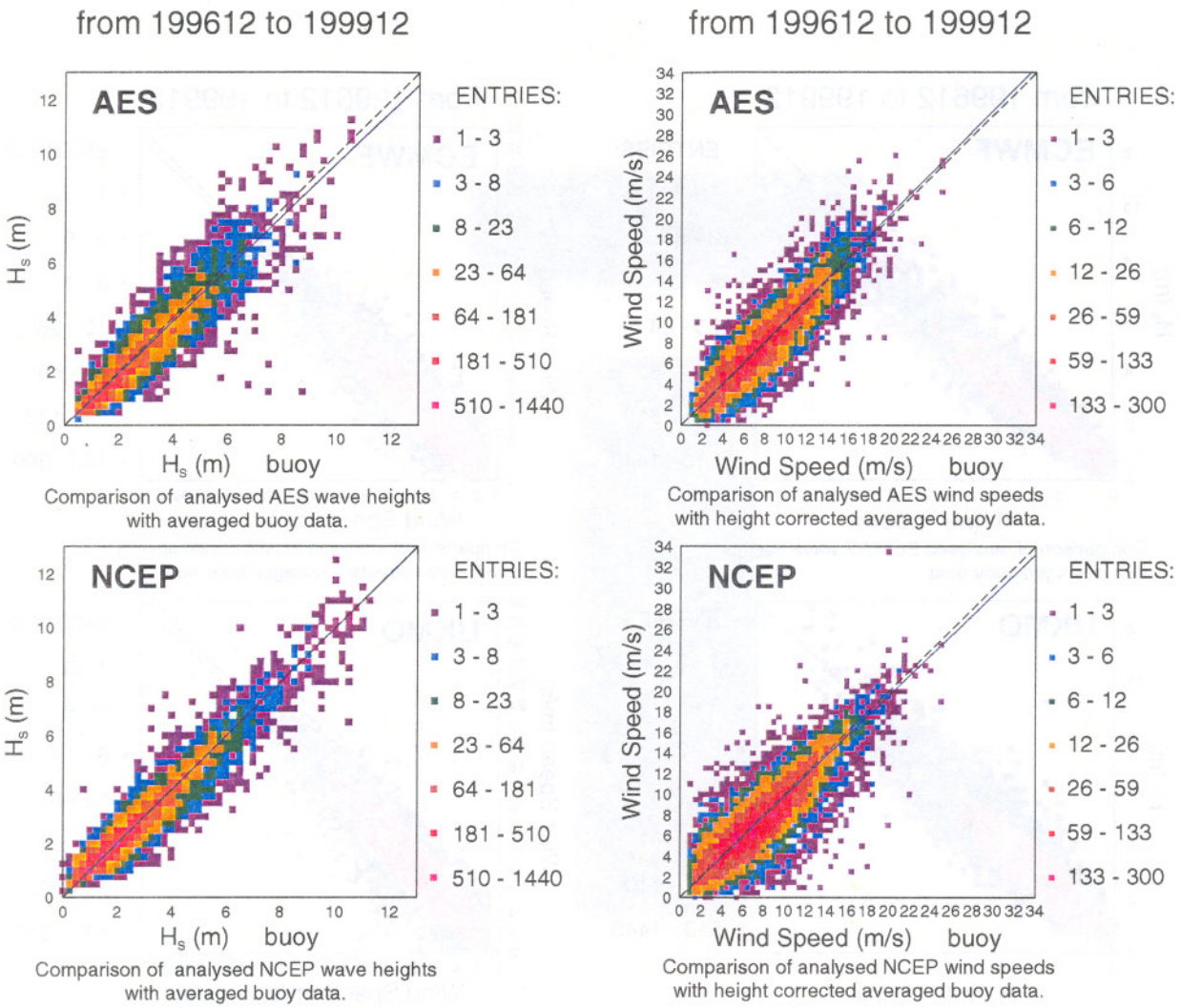

Figure 2b: Scatter diagrams for the 12Z analysed wave heights (left) and wind speeds (right) with respect to the averaged buoy data (see text). Buoy wind speeds were adjusted to 10m by using a neutrally stable logarithmic wind profile. Only buoys for which ECMWF, UKMO, and FNMOC model data were available were used to produce the statistics (figure 1). Note that AES results are limited to buoys along the American coasts and NCEP has reported less data points than the others. The solid line is the linear fit through the origin with a slope given by the symmetric slope (see tables).

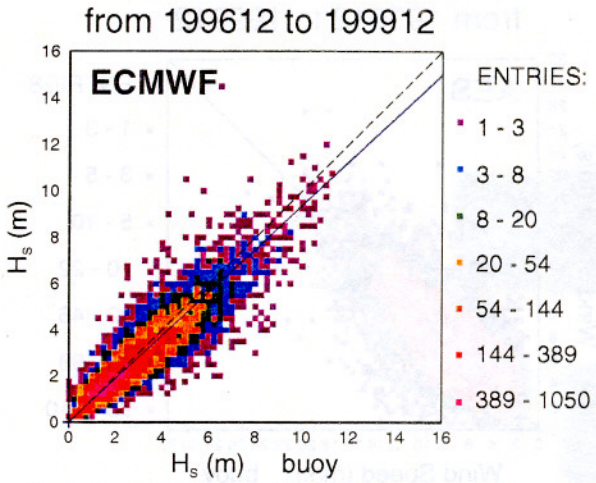

Comparison of forecast(t=t+2) ECMWF wave heights with averaged buoy data.

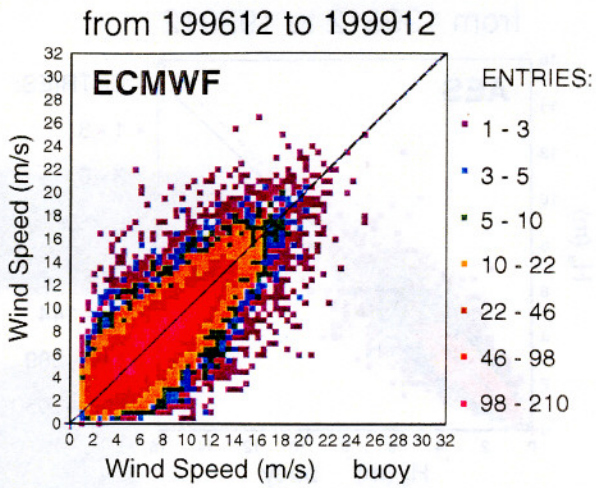

Comparison of forecast(t=t+2) ECMWF wind speeds with height corrected averaged buoy data.

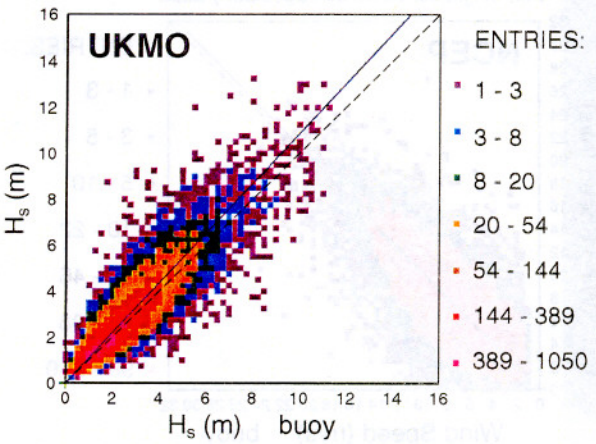

Comparison of forecast(t=t+2) UKMO wave heights with averaged buoy data

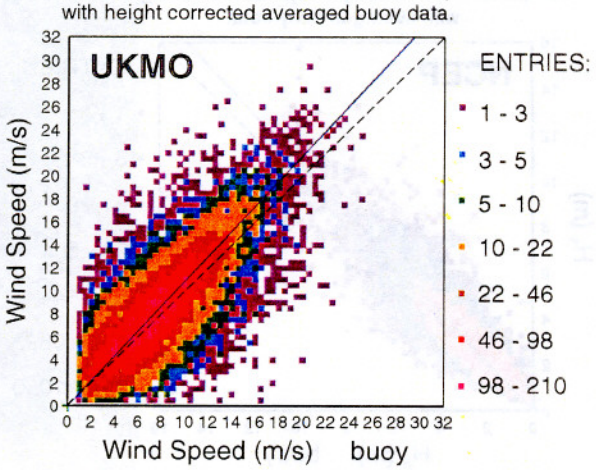

Comparison of forecast(t=t+2) UKMO wind speeds with height corrected averaged buoy data.

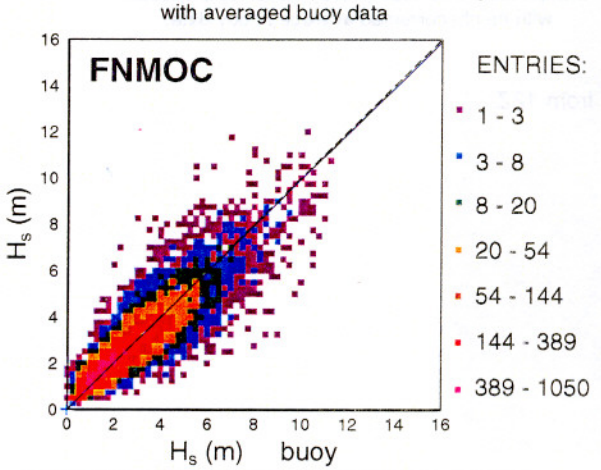

Comparison of forecast(t=t+2) FNMOC wave heights with averaged buoy data.

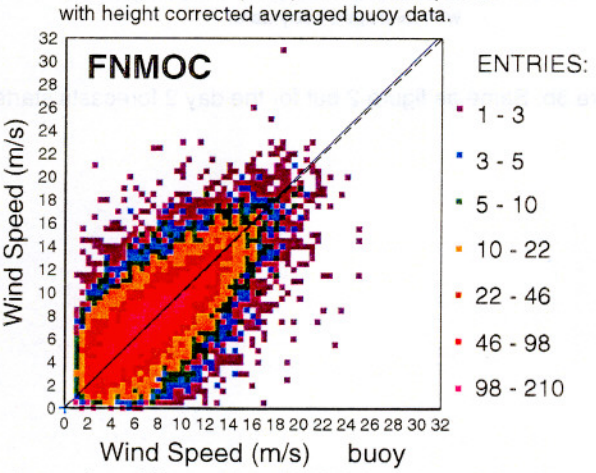

Comparison of forecast(t=t+2) FNMOC wind speeds with height corrected averaged buoy data.

Figure 3a: see figure 3b

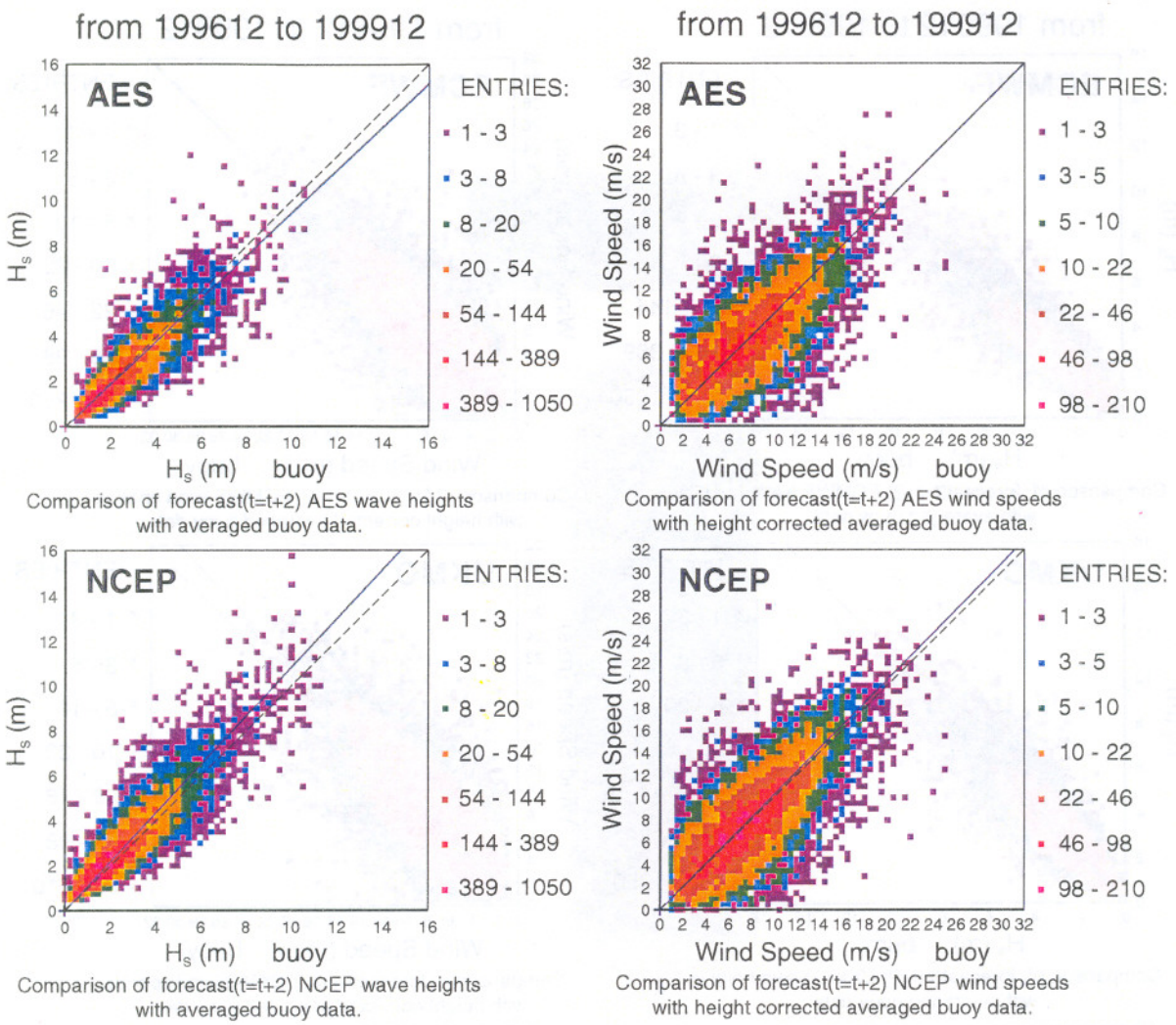

Figure 3b: Same as figure 2 but for the day 2 forecasts started from 12Z.

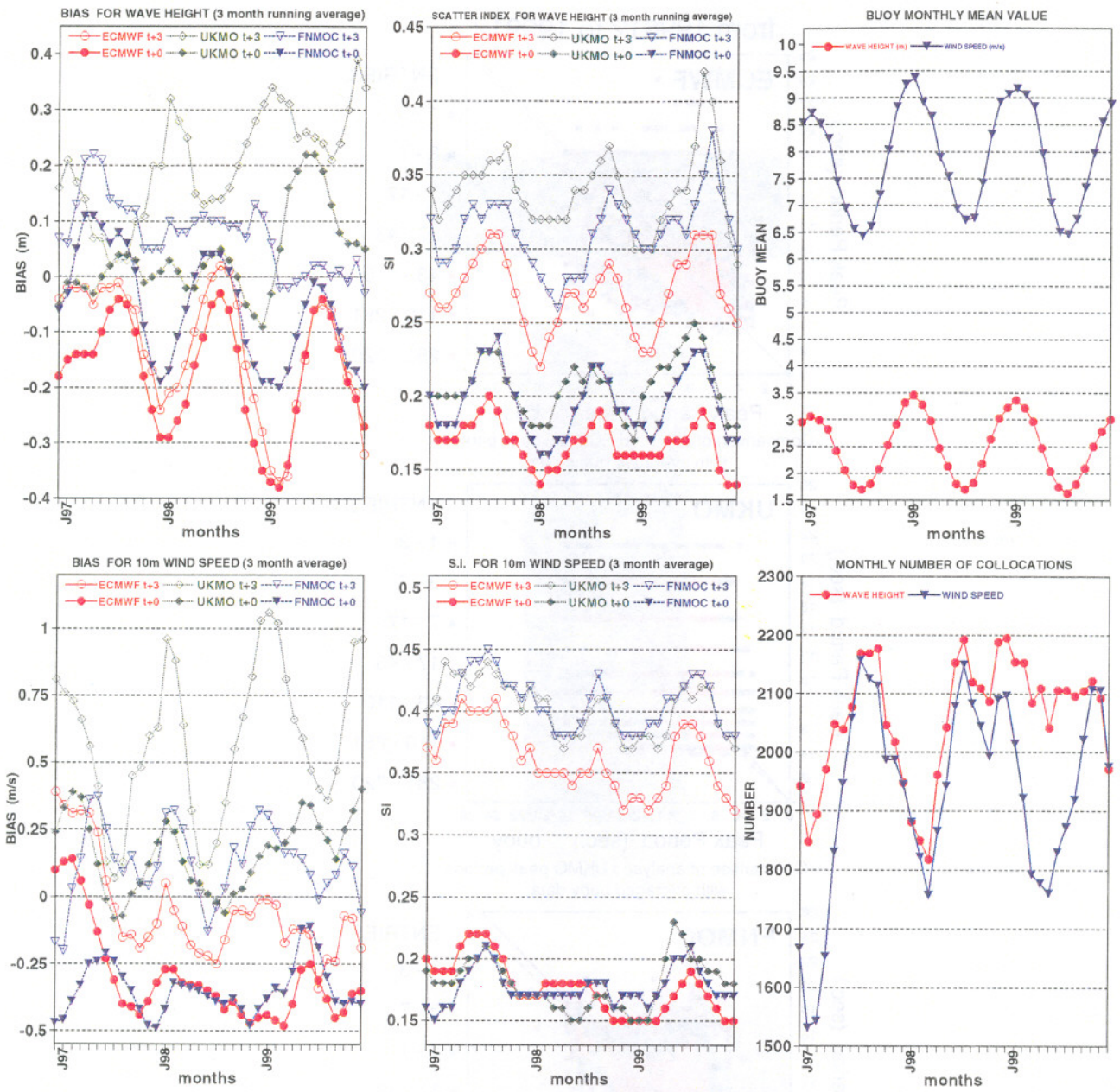

Figure 4: Monthly time series of analysis (t+0) and forecast day 3 (t+3) bias and scatter index for model wave heights and 10m winds when compared to buoy data which are common to ECMWF (solid red circles), UKMO (dot green diamonds), and FNMOC (dashed blue triangles) from December 1996 to December 1999. Buoy winds were adjusted to 10m and a 3 month running average was used to smooth out the plots. Also shown are the mean buoy observations and the number of collocations between models and buoys.

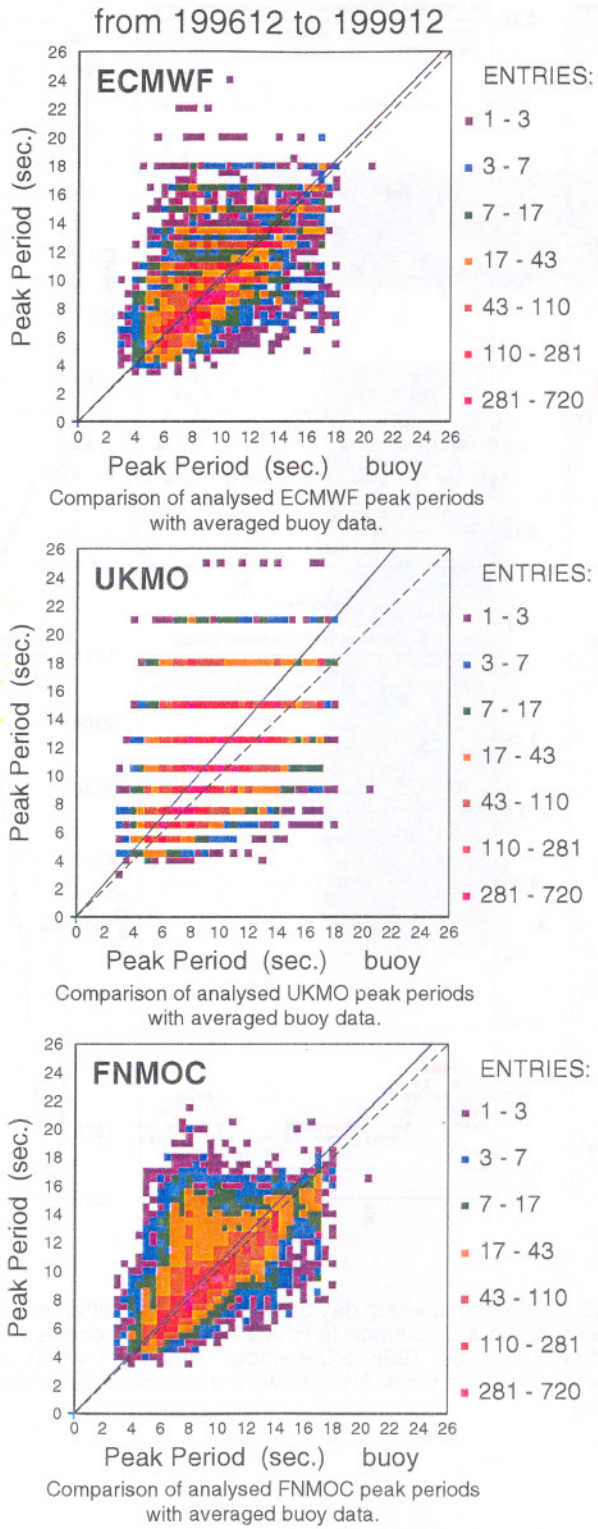

Figure 5: Same as figure 2 but for the period at the peak of the one-dimensional analysed wave spectra.

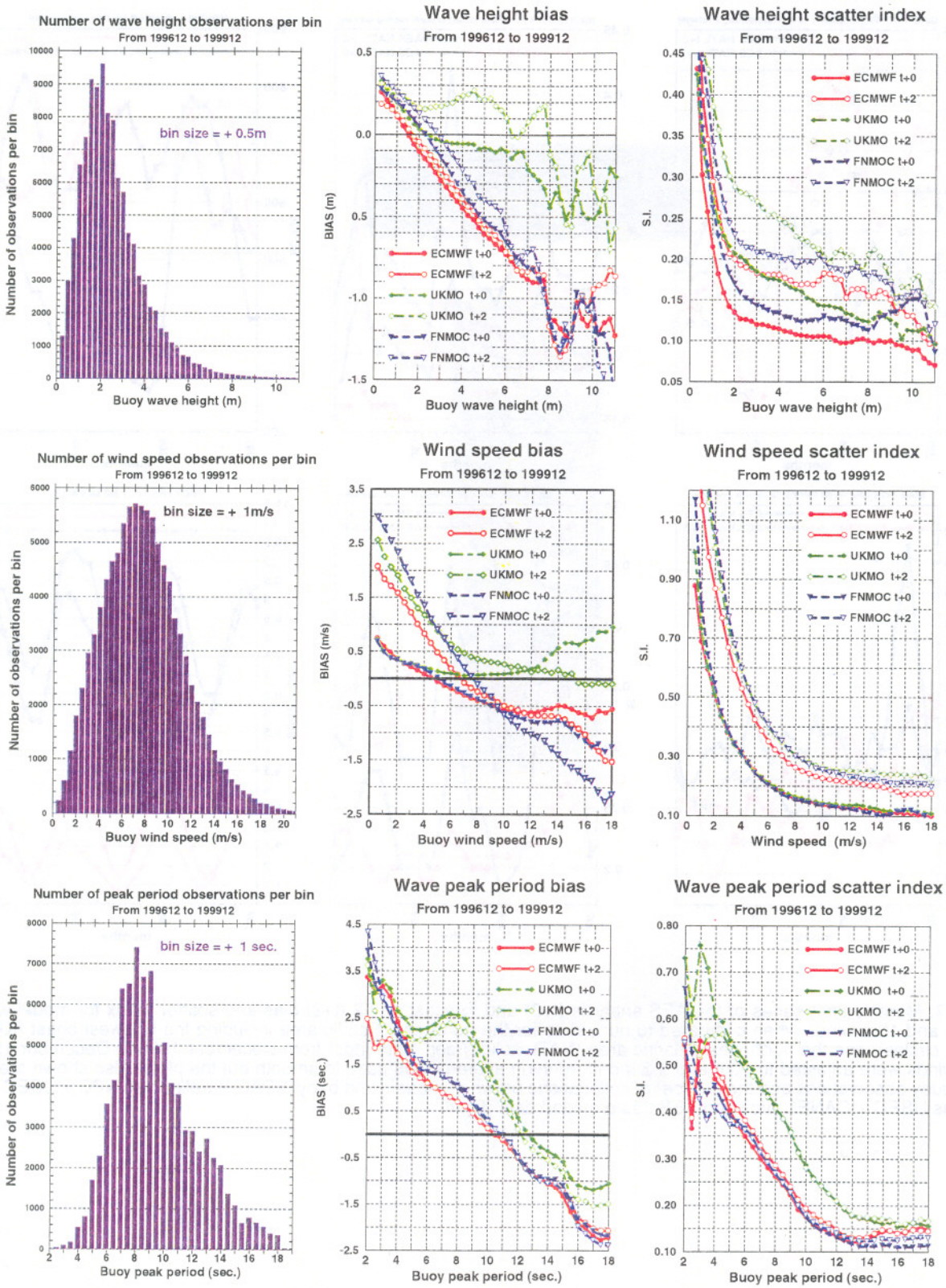

Figure 6: Bias and scatter index as obtained when data are binned with respect to the buoy data for the period from December 1996 to 1999. The number of observations per bin is also given. Note that the bins overlap. The same symbol and colour convention as in figure 4 is used.

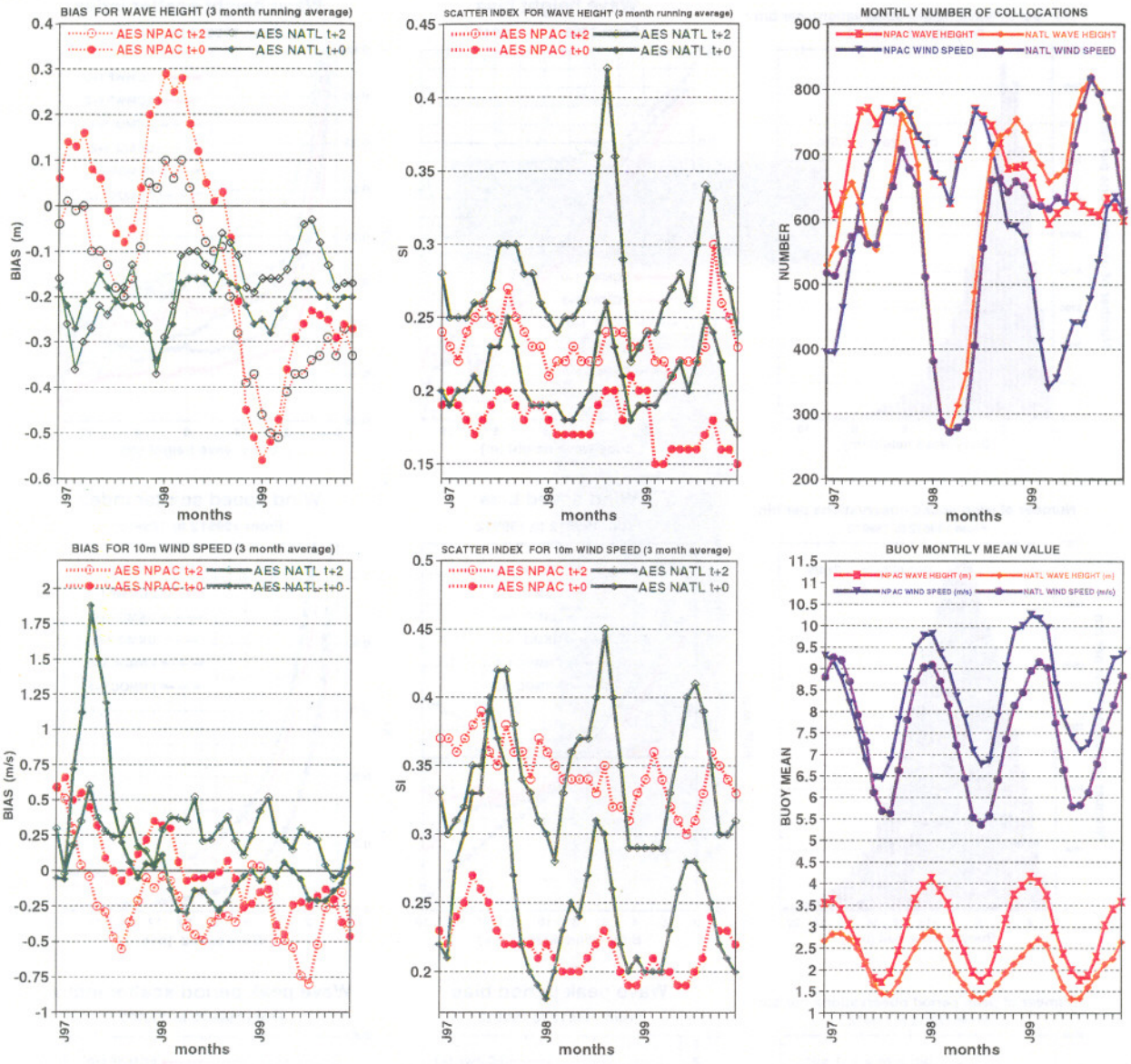

Figure 7: Monthly time series of the AES analysis (t+0) and forecast day 2 (t+2) bias and scatter index for model wave heights and 10m winds when compared to buoy data for the north east Pacific area including the US west coast (NPAC dot red circles), and the north west Atlantic area (NATL solid green diamonds) from December 1996 to December 1999. Buoy winds were adjusted to 10m and a 3 month running average was used to smooth out the plots. Also shown are the mean buoy observations and the number of collocations between models and buoy. NPAC is defined as NPC + USEC and NATL as USEC + CANEC provided AES has provided data (figure1).

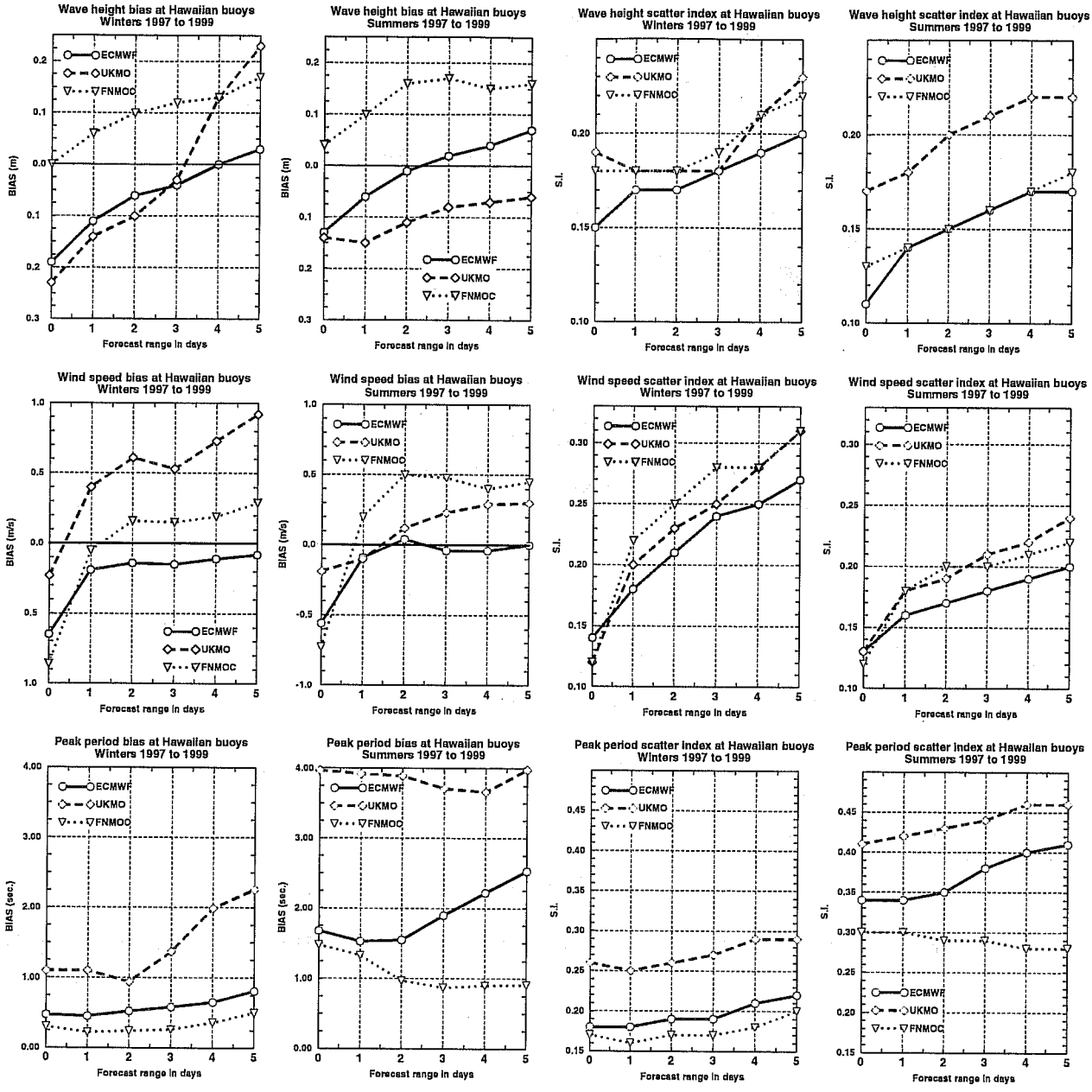

buoy statistics	number of entries in winter	winter mean	number of entries in summer	summer mean
wave height (m)	939	2.94	942	2.06
10m wind speed (m/s)	908	7.83	942	7.56
peak period (s)	911	11.74	941	8.81

Figure 8: Winter or summer biases and scatter indices at the Hawaiian buoys as a function of forecast range for wave heights, 10m wind speeds and peak periods from ECMWF, UKMO and FNMOC for the period from December 1996 to December 1999.

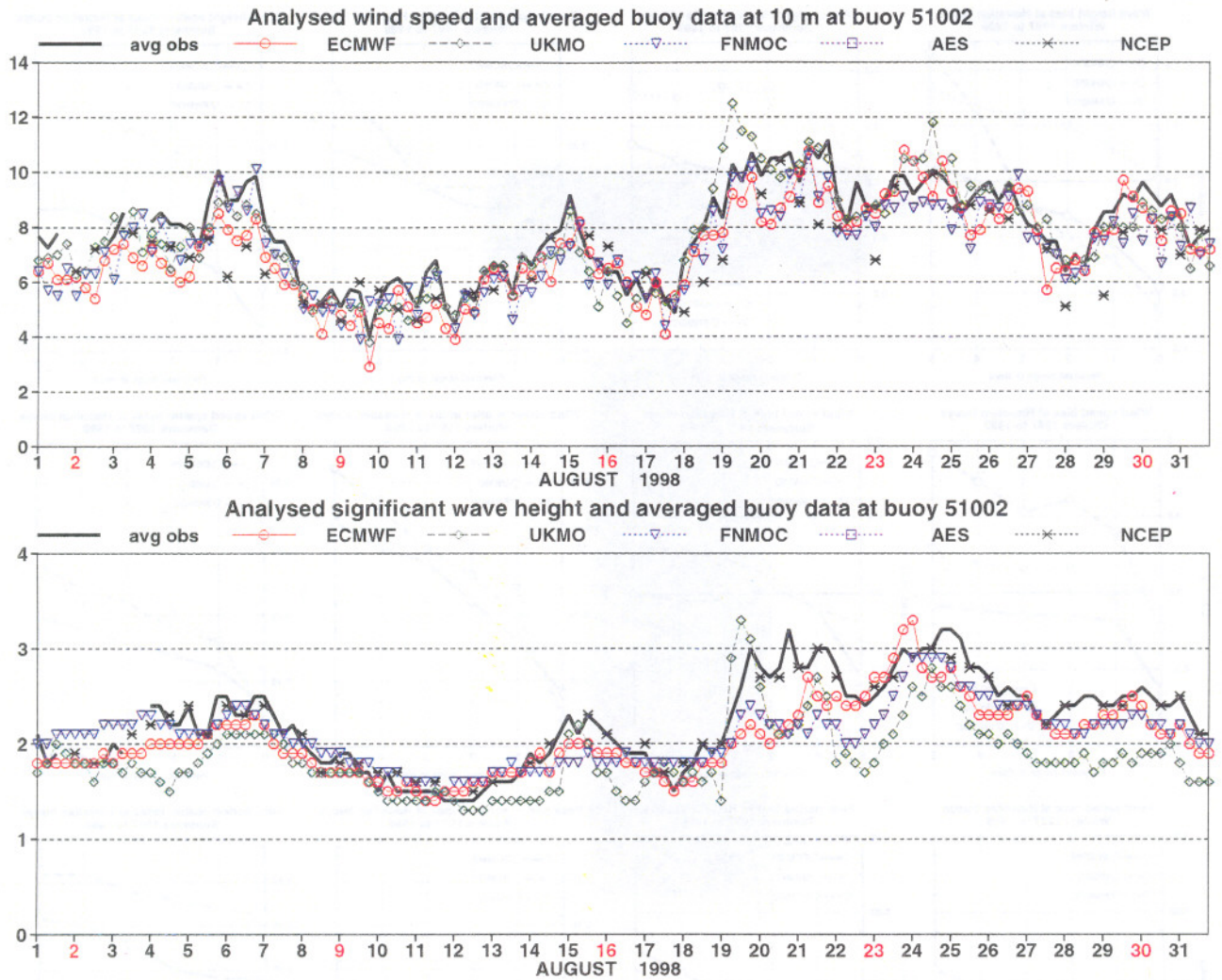

Figure 9: Time series of analysed 10m wind speed (m/s) and wave height (m) at buoy 51002 south west of Hawaii for the month of August 1998.

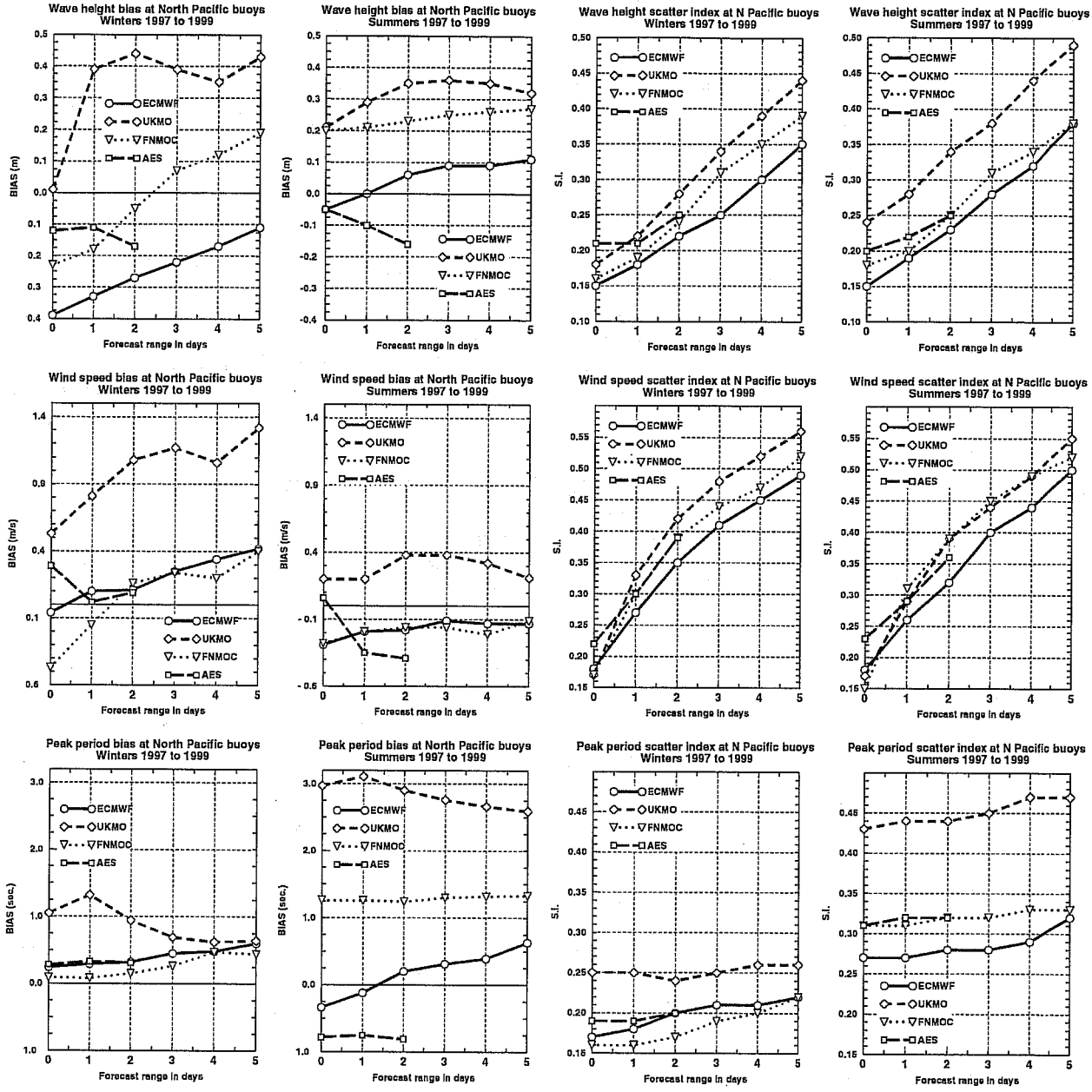

buoy statistics	number of entries in winter	winter mean	number of entries in summer	summer mean
wave height (m)	1165	3.88	1294	1.74
10m wind speed (m/s)	941	9.64	1202	6.70
peak period (s)	1159	11.31	1284	9.26

Figure 10: Winter or summer biases and scatter indices at buoys in the north eastern Pacific area as a function of forecast range for wave heights, 10m wind speeds and peak periods from ECMWF, UKMO, FNMOC and AES for the period from December 1996 to December 1999.

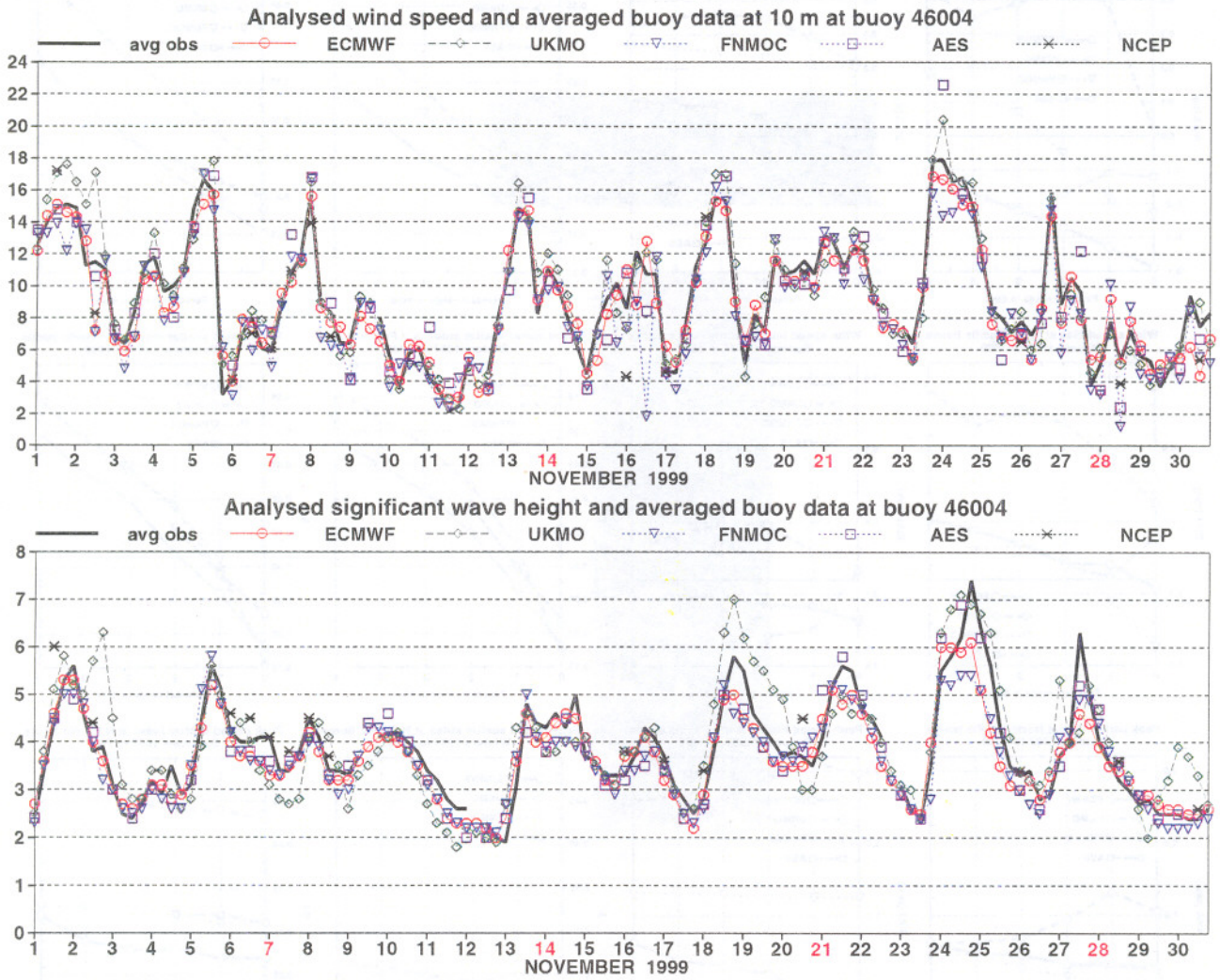

Figure 11: Time series of analysed 10m wind speed (m/s) and wave height (m) at buoy 46004 west of Vancouver Island for the month of November 1999.

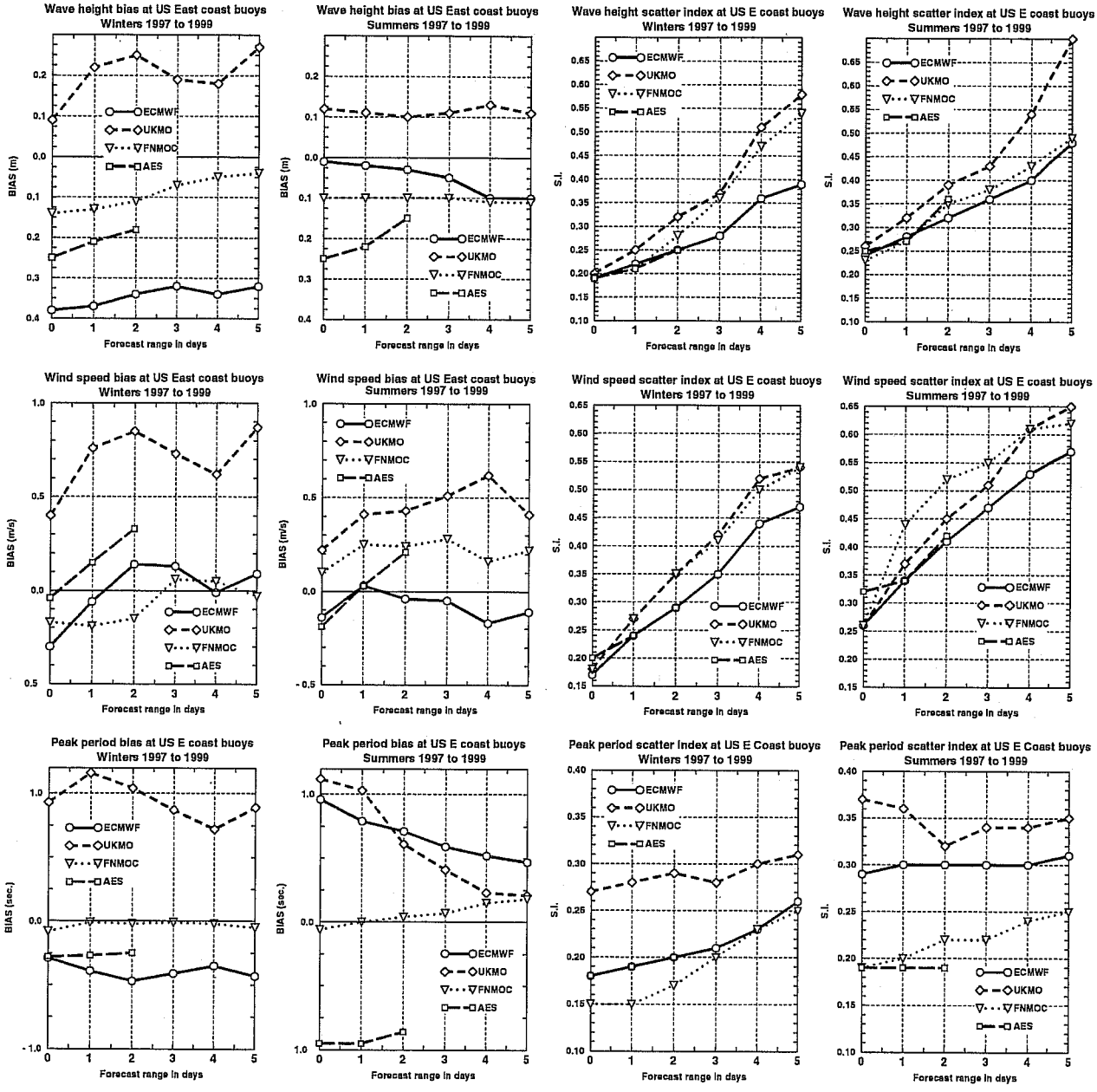

buoy statistics	number of entries in winter	winter mean	number of entries in summer	summer mean
wave height (m)	1052	2.44	1154	1.33
10m wind speed (m/s)	1020	8.68	1111	5.58
peak period (s)	1052	8.47	1150	7.34

Figure 12: Winter or summer biases and scatter indices at buoys along the eastern US coast as a function of forecast range for wave heights, 10m wind speeds and peak periods from ECMWF, UKMO, FNMOC and AES for the period from December 1996 to December 1999.

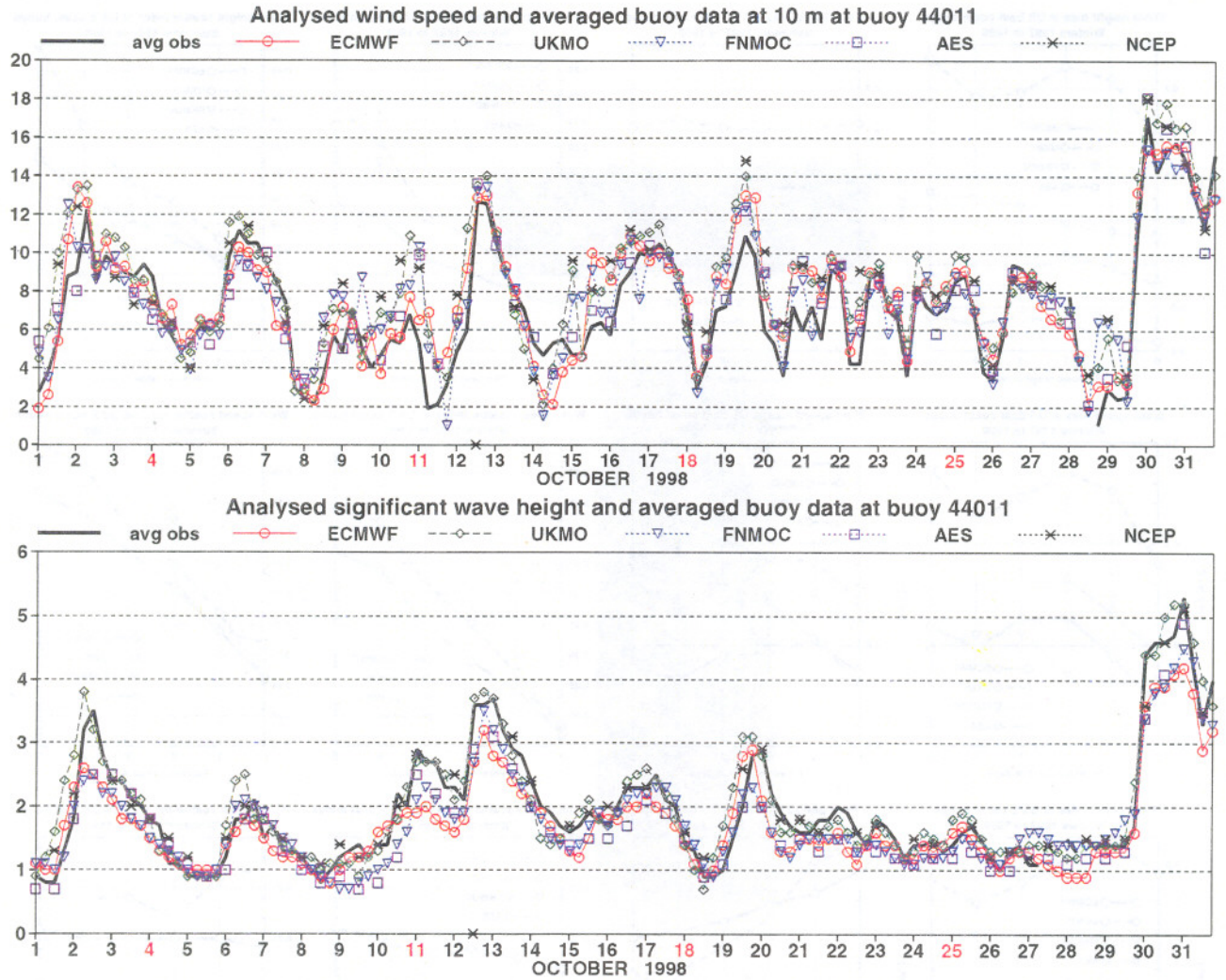

Figure 13: Time series of analysed 10m wind speed (m/s) and wave height (m) at buoy 44011 on the Georges Bank east of Cape Cod for the month of October 1998.

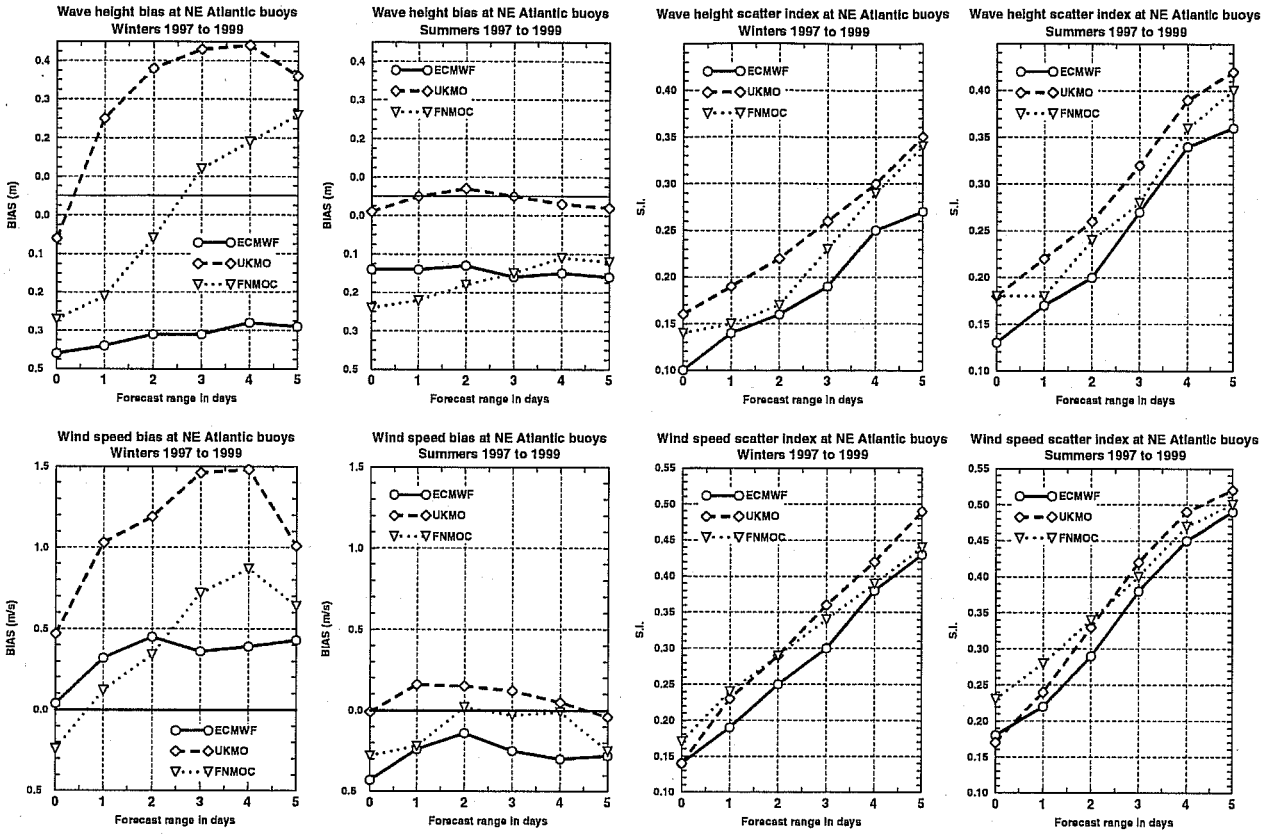

buoy statistics	number of entries in winter	winter mean	number of entries in summer	summer mean
wave height (m)	968	4.55	1060	2.22
10m wind speed (m/s)	931	10.76	1036	7.52

Figure 14: Winter or summer biases and scatter indices at buoys west of the British Isles as a function of forecast range for wave heights, 10m wind speeds and peak periods from ECMWF, UKMO and FNMOC for the period from December 1996 to December 1999.

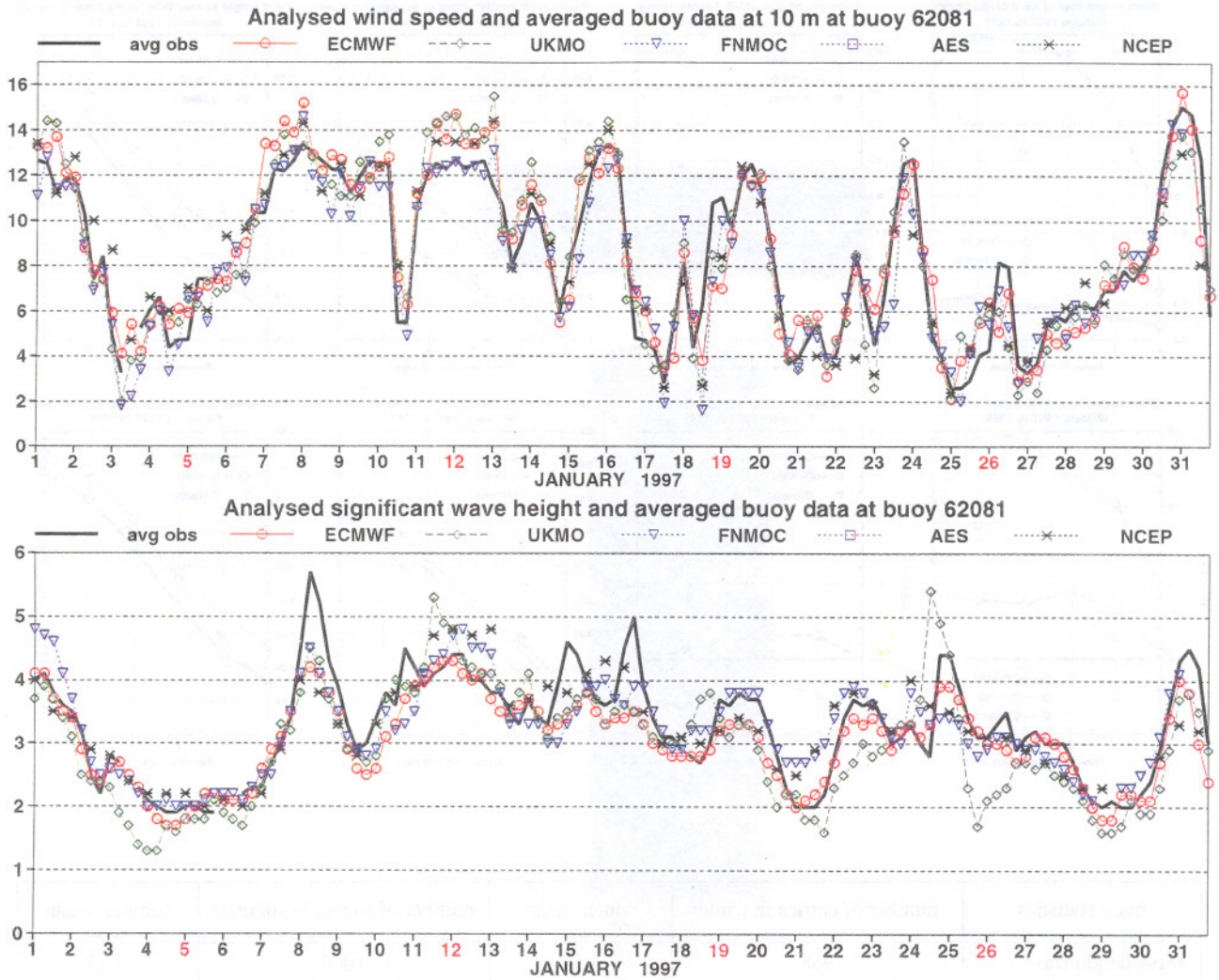

Figure 15: Time series of analysed 10m wind speed (m/s) and wave height (m) at buoy 62081 south west of Ireland for the month of January 1997.

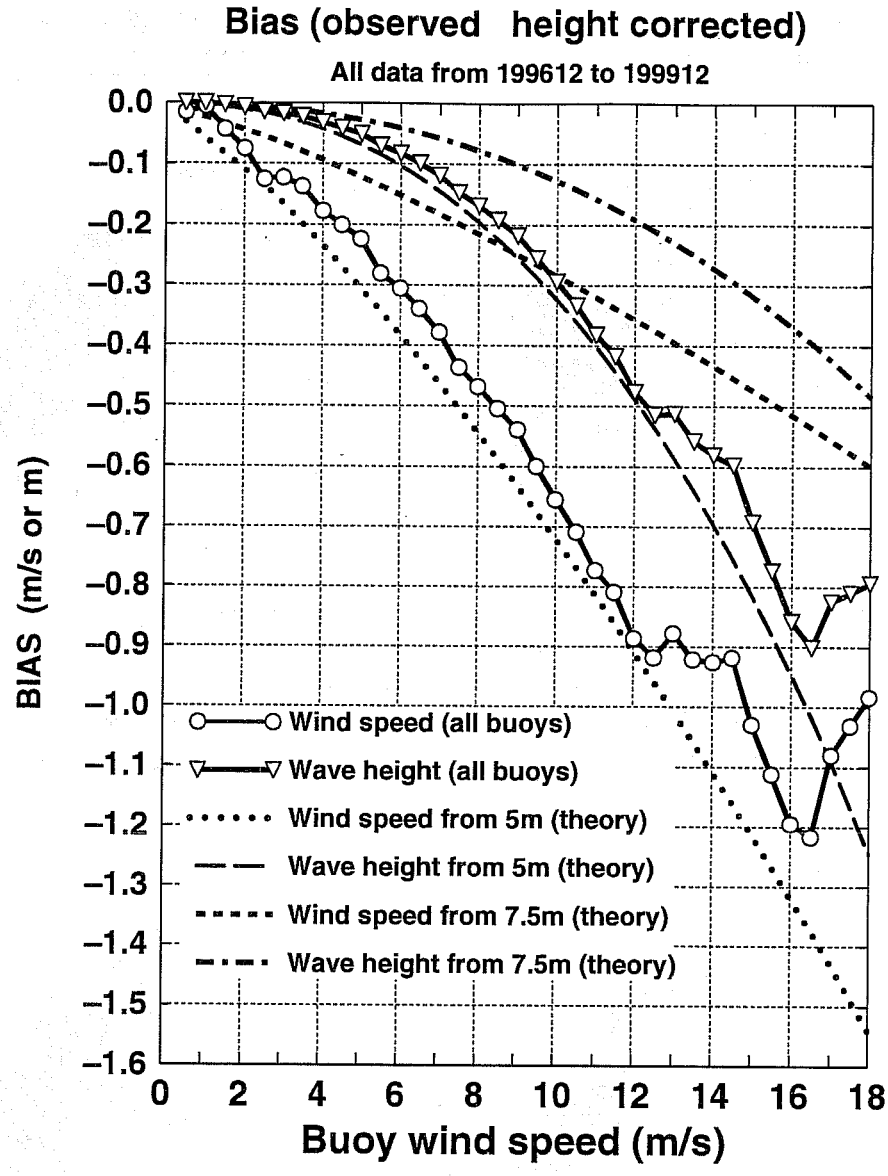

Figure 16: The solid lines with circles displays the difference between the 10m wind speed bias (as in figure 6) and the bias that was obtained when the buoy data were not adjusted for the actual anemometer height. The solid line with triangles is derived from the previous relation using formula (2). The dotted line is showing the difference in wind speed at 5m and 10m as a function of the wind speed at 5m. The long-dashed line the corresponding bias in wave height according to (2). The short-dashed line is the wind speed difference between 7.5m and 10m as a function of the wind at 7.5m and the dot-dashed line the corresponding bias in wave height according to (2).

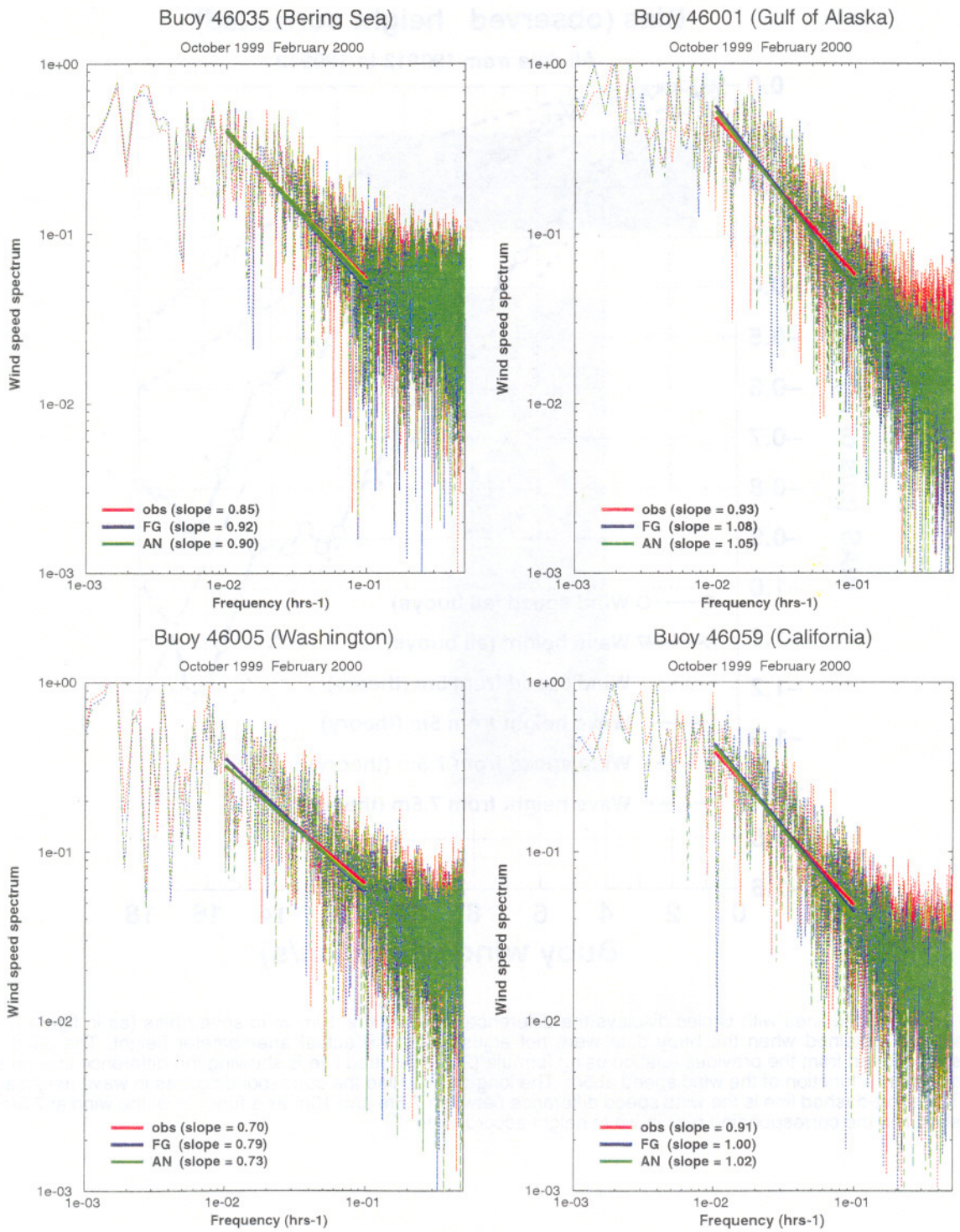

Figure 17: 10m wind speed frequency spectra from hourly time series of model first guess (blue line), model analysis (green line) and observations at buoy location along the US West Coast and Alaska. Buoy data were adjusted to 10m (see text). The solid lines are the linear fit to the slope between 100 to 10 hours.

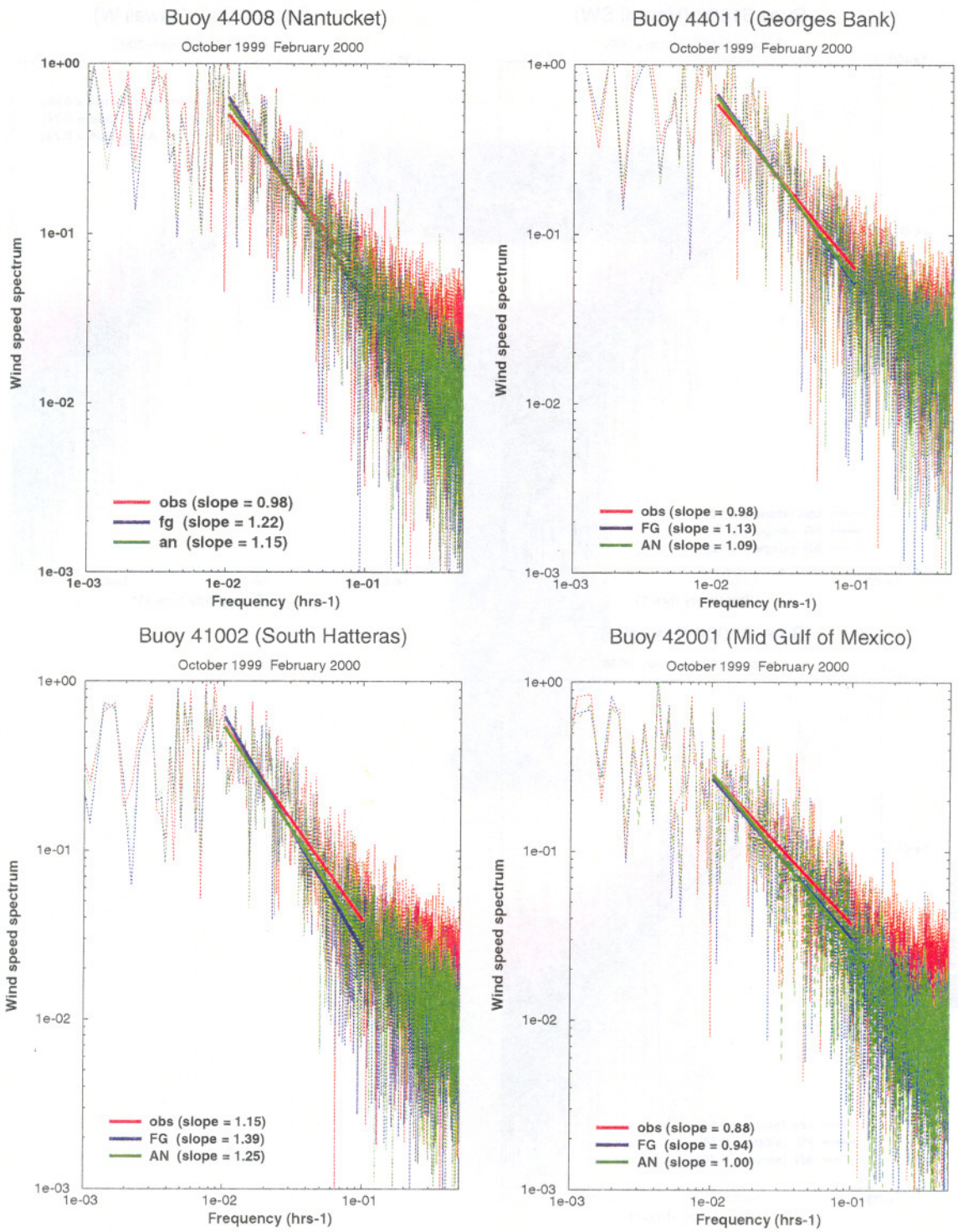

Figure 18: 10m wind speed frequency spectra from hourly time series of model first guess (blue line), model analysis (green line) and observations at buoy location along the US East Coast and the Gulf of Mexico. Buoy data were adjusted to 10m (see text). The solid lines are the linear fit to the slope between 100 to 10 hours.

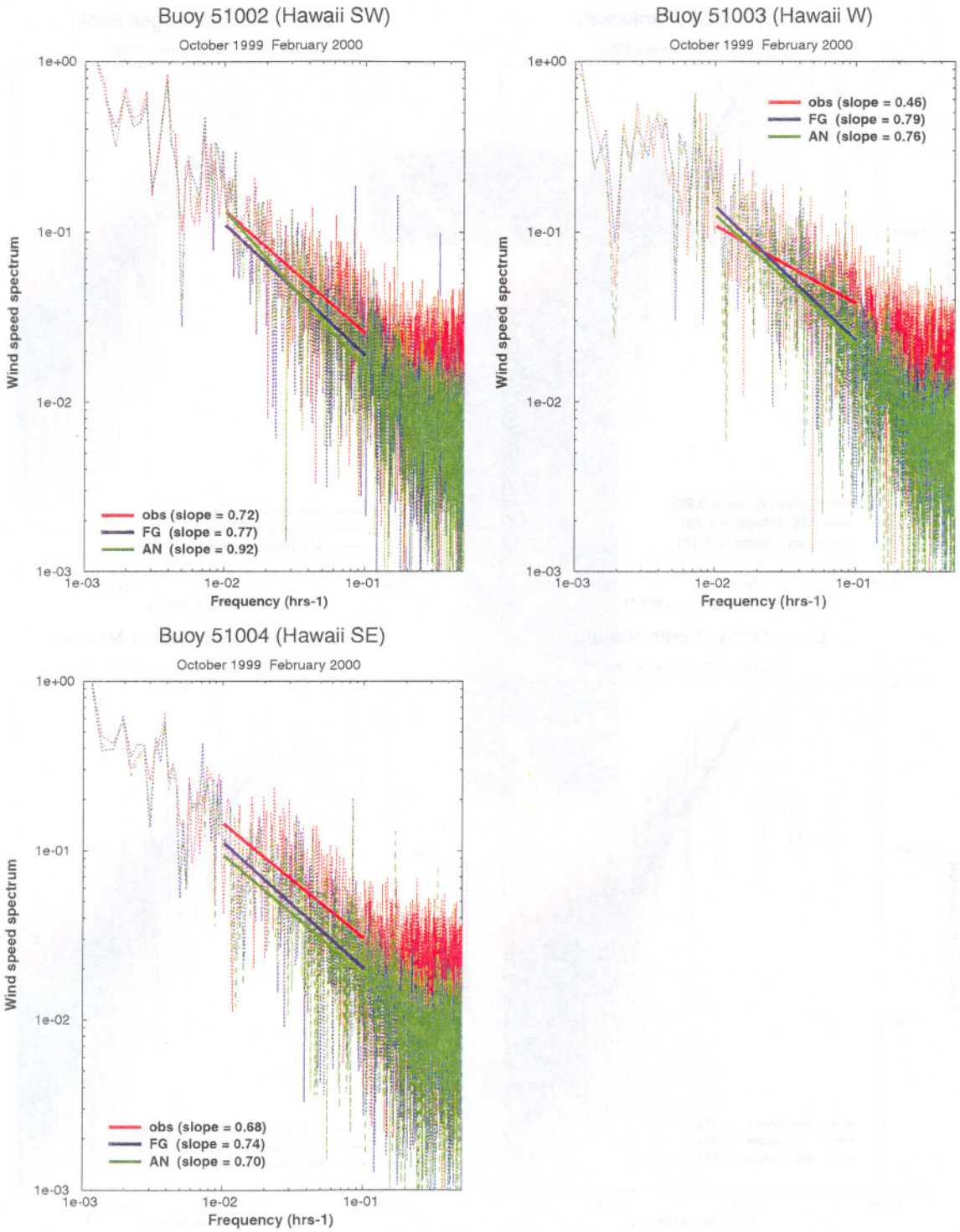

Figure 19: 10m wind speed frequency spectra from hourly time series of model first guess (blue line), model analysis (green line) and observations at buoy location in the vicinity of the Hawaiian Islands. Buoy data were adjusted to 10m (see text). The solid lines are the linear fit to the slope between 100 to 10 hours.